Title
Oxygen and food modulate Caenorhabditis elegans locomotory circuits

Author
Gray, Jesse M

Publication Date
2005

Peer reviewed|Thesis/dissertation

Oxygen and Food Modulate *C. elegans* Locomotory Circuits

by

Jesse M. Gray

DISSERTATION

Submitted in partial satisfaction of the requirements for the degree of

DOCTOR OF PHILOSOPHY

in

Biochemistry

in the

GRADUATE DIVISION

of the

UNIVERSITY OF CALIFORNIA, SAN FRANCISCO

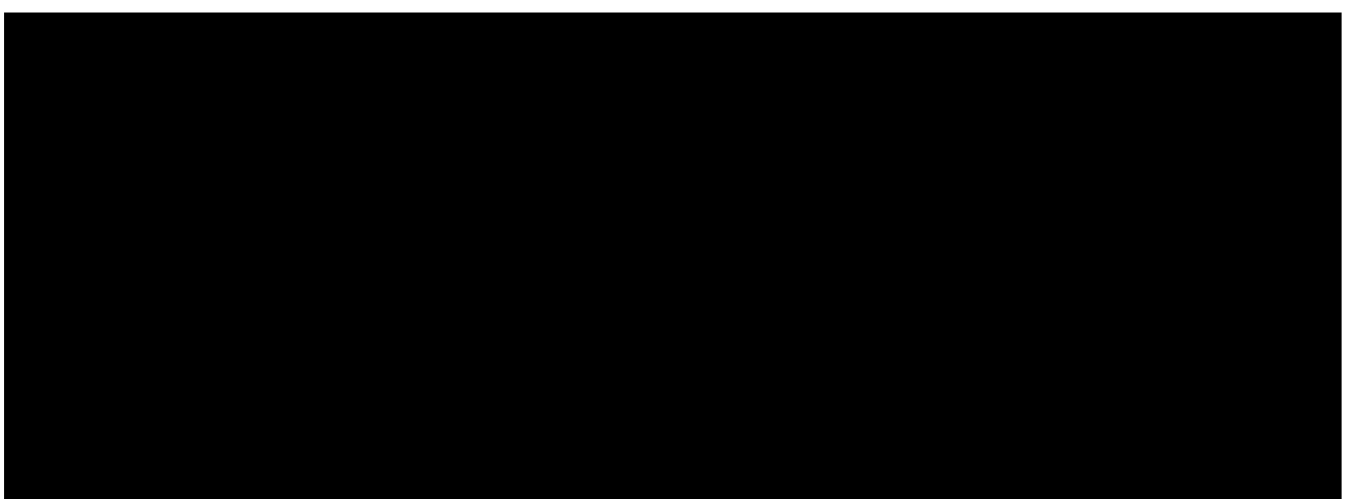

Date University Librarian

Degree Conferred:.....

Dedication

I dedicate this thesis to my parents and siblings, whom I love dearly. My parents taught me that anything in life is possible if you set your mind to it. When they saw that I had taken this lesson too literally, they helped me to understand that it is also wise to appreciate one's limits. Others who know me well can attest that I have been refractory to this second lesson, and I would like to make it clear that it is not because my parents did not make every effort. Mainly, without their support and encouragement throughout my life, this thesis would not have been possible.

Acknowledgements

I acknowledge good friends from outside the lab. Aylin Rodan, a brilliant classmate and happy companion, that rare person who appreciates every form of pleasure but also has rock-hard discipline. Linus Tsai, whose humble attitude reflects our humility in the face of mother nature and whom, along with roommate Genevieve Preer, I hold as the ultimate model for how to be a good parent. Nate Medbery who helped me through 9th grade sludge lab and timidly joined me at my first high school dance; Nate and the ever practical Bob Plankers who visited San Francisco frequently, once in the Sea Bass. Bab!... Jeanne and Randy, the best roomies ever. My aunt Lisa and uncle Tom, who fully understand why California is the best. My aunt Pat and uncle Mike, who know that New York is superior.

The larger Bargmann lab is like a family and was most so to me in the beginning. The annex a family within a family. Mario de Bono, my rotation advisor, teaching me basic techniques by working side-by-side with me until I understood. He also made it clear that science at its best should be fun, a lesson all too often forgotten. Mike Galko, from whom I learned that life is "Pure gravy. And don't forget it." Christelle Sabatier, with a remarkable sense of *Sophrosyne*. Sue Kirch, pure fun and enthusiasm. Hwai Jong, whose reluctance to fully grow up is an unusual gift.

Outside the annex, Zemer Gitai, a great source of energy and wit. Amanda Kirby-Kahn, Kirby at the time, a fun-injector. David Tobin, a liberal's liberal. Noelle L'Etoile, the

sweetest person in the whole wide world. Carrie Adler, as different from me as is possible, but we both went through everything together like brother and sister. Miri VanHoven: words cannot describe how good a person she is. Greg Lee, too calm for life.

Special people. Sreekanth Chalasani, like a brother. One of the sweetest, most considerate, most amazing human beings on the planet. Despite his unassuming nature, a wealth of knowledge and insight. Hang Lu, where all the same notes apply, but what a delicious flirt! Yuuuuuuuin! Manny! And Massimo Antonio Hilliard!

David Karow and Steve McCarroll, a category of their own. David was the ultimate intellectual source of the most exciting experiments I have ever performed. He asked a simple question, why does *C. elegans* have seven soluble guanylate cyclases and no nitric oxide synthase. This question led to the most exciting experiments I have ever performed. Steve was one of the brightest independent sources of brilliance within the lab, and it was important for me to see what independent brilliance looked like. The best part was the so-called triumvirate, which was the magic that happened when David and Steve and I gathered together after a day of experiments. It was as though we were the three missing pieces of a puzzle, everything fluid and exciting but right and secure at the same time.

I thank Michael Marletta, who was a spectacular advisor to David Karow and who was an enormously positive force in the development of our collaborative project involving

sGCs in oxygen-sensing and behavior, initiating the collaboration and keeping it focused. Michael Marletta is also an outstanding human being.

I thank Cori, whose intellect dominates the lab and whose creativity, clarity of thought, and vast store of accessible knowledge are unparalleled. Beyond the intellectual, there was a constant theme for me in graduate school of observing the problems encountered by my classmates and friends and appreciating that so often these were the sorts of troubles that simply did not crop up in Cori's lab. So in addition to brilliance, I have to credit Cori with great management. I experienced that great management personally many times, when Cori's comments seemed to be tailored specifically to what I needed or my project needed at the time. To have been able to learn from a true master is one of the great pleasures of my life.

I also want to thank my thesis and orals committees, composed of Graeme Davis, Ulrike Heberlein, Philip Sabes, David Agard, and Cori Bargmann. My orals committee in particular was instrumental in doing the hard work to help me start thinking more in specific and concrete terms rather than in vague, ungrounded ones.

I thank Holly Hunnicutt, whose wit and humor and general level of strangeness more than kept me on my toes!

Finally, I want to thank Justine, who is my partner, my lover, my companion, and my scientific advisor – and who makes it all worthwhile.

Previously Published Work and Contributions

Chapter 2 of this thesis is a reproduction of a manuscript entitled, "A circuit for navigation in *C. elegans*," by Jesse M. Gray, Joseph J. Hill, and Cornelia I. Bargmann, published in *The Proceedings of the National Academy of the United States of America* 2005; 102(9)3184-91. Chapter 3 of this thesis is a reproduction of a manuscript entitled, "oxygen sensation and social feeding mediated by a *C. elegans* guanylate cylcase homolog," by Jesse M. Gray and David S. Karow (co-first authors), Hang Lu, Andy J. Chang, Jennifer S. Chang, Ronald E. Ellis, Michael A. Marletta, and Cornelia I. Bargmann, published in *Nature* 2004 430(6997)317-22. It is reprinted by permission from Macmillan Publishers Ltd: *Nature* 430 (6997)317-22, copyright 2005. Parts of the abstract of this dissertation were taken or adapted from the above two manuscripts.

Figure 1 of Chapter 3 was done by Hang Lu. Figure 3 of Chapter 3 was done by David Karow. Figures 2, 4, and 5 of Chapter 3 were done collaboratively by Jesse Gray and David Karow, with Cori Bargmann performing the cell identification in Figure 2. Supplemental Figure 2 of Chapter 3 was done by Hang Lu and Cornelia Bargmann. Panels A and B of Supplemental Figure 3 of Chapter 3 were done by Hang Lu and Andy Chang, respectively. Figure 5C in Chapter 3 was done by Hang Lu. Some experiments in Chapter 2 were done both by Jesse Gray and Joseph Hill. A few experiments in Chapter 2 may have been done by Joseph Hill alone. Some plasmids from Chapter 4 were provided by Martin Hudson and David Morton. The remainder of this thesis was carried out by Jesse M. Gray in collaboration with and under the supervision of Cornelia I. Bargmann.

Copyright Permissions for Chapter 1

Quoted from http://www.pnas.org/misc/rightperm.shtml:

"PNAS authors need not obtain permission for the following cases: (1) to use their original figures or tables in their future works; (2) to make copies of their papers for their own personal use, including classroom use, or for the personal use of colleagues, provided those copies are not for sale and are not distributed in a systematic way; *(3) to include their papers as part of their dissertations;* or (4) to use all or part of their article in a printed compilation of their own works. Citation of the original source must be included and copies must include the copyright notice of the original report."

"Anyone may, without requesting permission, use original figures or tables published in PNAS for noncommercial and educational use (i.e., in a review article, in a book that is not for sale) provided that the original source and copyright notice are cited."

Copyright Permissions for Chapter 2

NATURE PUBLISHING GROUP LICENSE

TERMS AND CONDITIONS

Dec 07, 2005

Licensed content title

Oxygen sensation and social feeding mediated by a *C. elegans* guanylate cyclase homologue

Licensed content authors

Jesse M. Gray, David S. Karow, Hang Lu, Andy J. Chang, Jennifer S. Chang et al.

This is a License Agreement between Jesse M. Gray ("You") and Nature Publishing Group ("Nature Publishing Group"). The license consists of your order details, the terms and conditions provided by Nature Publishing Group, and the payment terms and conditions.

License Number	1363750249083
License date	Dec 07, 2005
Licensed content publisher	Nature Publishing Group
Licensed content publication	Nature
Year of publication	2004
Portion used	Full paper
Requestor type	Student
Type of Use	Thesis/Dissertation
Total Fee	$0.00

Terms and Conditions

Terms and Conditions for Permissions

Nature Publishing Group hereby grants you a non-exclusive license to reproduce this material for this purpose, and for no other use, subject to the conditions below:

1. NPG warrants that it has, to the best of its knowledge, the rights to license reuse of this material. However, you should ensure that the material you are requesting is original to Nature Publishing Group and does not carry the copyright of another entity (as credited in the published version). If the credit line on any part of the material you have requested indicates that it was reprinted or adapted by NPG with permission from another source, then you should also seek permission from that source to reuse the material.

2. Permission granted free of charge for material in print is also usually granted for any electronic version of that work, provided that the material is incidental to the work as a whole and that the electronic version is essentially equivalent to, or substitutes for, the print version.

Where print permission has been granted for a fee, separate permission must be obtained for any additional, electronic re-use (unless, as in the case of a full paper, this has already been accounted for during your initial request in the calculation of a print run).

NB: In all cases, web-based use of full-text articles must be authorized separately through the 'Use on a Web Site' option when requesting permission.

3. Permission granted for a first edition does not apply to second and subsequent editions and for editions in other languages (except for signatories to the STM Permissions Guidelines, or where the first edition permission was granted for free).

4. Nature Publishing Group's permission must be acknowledged next to the figure, table or abstract in print. In electronic form, this acknowledgement must be visible at the same time as the figure/table/abstract, and must be hyperlinked to the journal's homepage.

5. The credit line should read:

Reprinted by permission from Macmillan Publishers Ltd: [JOURNAL NAME] (reference citation), copyright (year of publication)

For AOP papers, the credit line should read:

Reprinted by permission from Macmillan Publishers Ltd: [JOURNAL NAME], advance online publication, day month year (doi: 10.1038/sj.[JOURNAL ACRONYM].XXXXX)

6. Adaptations of single figures do not require NPG approval. However, the adaptation should be credited as follows:

Adapted by permission from Macmillan Publishers Ltd: [JOURNAL NAME] (reference citation), copyright (year of publication)

7. Translations of up to a whole article do not require NPG approval. The translation should be credited as follows:

Translated by permission from Macmillan Publishers Ltd: [JOURNAL NAME] (reference citation), copyright (year of publication)

We are certain that all parties will benefit from this agreement and wish you the best in the use of this material. Thank you.

Abstract

Oxygen and Food Modulate *C. elegans* Locomotory Circuits

Jesse. M. Gray

C. elegans is a simple model system in which behavior can be studied from sensory input to motor output. Despite this potential, many elements of *C. elegans* behavior are not understood. Poorly understood areas include (1) how locomotory behaviors are influenced by food and (2) how locomotory behaviors are influenced by oxygen.

To understand how food influences locomotion, we observed animals on and off food, and we used laser kills to identify neurons involved in these behaviors. After animals are removed from bacterial food, they initiate a local search behavior consisting of reversals and omega turns triggered by AWC olfactory neurons, ASK gustatory neurons, and AIB interneurons. Over the following 30 minutes, the animals disperse as reversals and omega turns are suppressed by ASI gustatory neurons and AIY interneurons. Downstream interneurons and motor neurons encode specific aspects of reversal and turn frequency, amplitude, and directionality. Many of these neurons are also implicated in chemotaxis and thermotaxis. Thus this circuit may represent a common substrate for multiple navigation behaviors.

To understand how *C. elegans* sense and respond to oxygen, we subjected animals to spatial and temporal oxygen gradients. We found that the *C. elegans* exhibits a behavioural preference for 5-12% oxygen. Avoidance of high oxygen requires the

sensory cGMP-gated channel *tax-2/tax-4* and the soluble guanylate cyclase homolog *gcy-35*. The GCY-35 heme domain binds molecular oxygen, unlike the heme domains of classical guanylate cyclases. GCY-35 and TAX-4 act in four sensory neurons that control a naturally polymorphic social feeding behaviour in *C. elegans*. Social feeding occurs only when oxygen exceeds *C. elegans*' preferred level and requires *gcy-35*. Our results suggest that soluble guanlyate cyclases are a novel class of oxygen sensors and that social feeding can be a behavioural strategy for responding to hyperoxic environments.

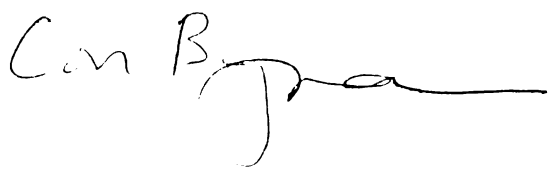

Table of Contents

List of Tables

List of Figures

Chapter 1 – Introduction

Assembling Neural Circuits in C. elegans

This thesis (Chapter 2) attempts to identify the neurons that comprise a circuit for navigation in *C. elegans*. Complete circuits are difficult to define because they are often too complex to map anatomically. In *C. elegans*, we have a complete wiring diagram (White, 1986), but even in such a simple and anatomically defined system there are barriers to functionally mapping circuitry. One difficulty involves the complexity of distributed systems, where individual neurons often only play a small part in a behavior. Another problem is that many neurons release multiple neurotransmitters, which can have different, even opposite, effects. Finally, complex behaviors are often made up of individual steps, which have to be dissected before functional circuits can be understood. Only one circuit in *C. elegans*, a circuit for simple responses to touch (Chalfie et al., 1985), is by any reasonable definition completely defined. Several behavioral circuits in *C. elegans* are partially delineated, including those for male mating, egg-laying, ASH-mediated avoidance of noxious stimuli, slowing on food, chemotaxis, and thermotaxis. Each of these is briefly described below.

The best understood circuit in *C. elegans* is the touch circuit, described in the introduction to Chapter 2. Briefly, touch-sensing neurons synapse onto the command neurons, which innervate dozens of motor neurons along the body and are required for backward (AVA and AVD) and forward (PVC and AVB) movement (Chalfie et al., 1985). The command neurons are likely to make the decision to move forward or backward (Maricq et al., 1995; Zheng et al., 1999).

The command neurons are important beyond their role in touch. Their role in forward and backward movement makes them relevant to any behavior that involves movement of the whole animal. Sensory neuron output can be traced in one to four hops to the command neurons (Chalfie et al., 1985). Neurons involved in sensing repulsive stimuli, such as ASH (Hart et al., 1995; Maricq et al., 1995) or AWB (Troemel et al., 1997), often synapse directly onto the command neurons, while neurons that sense attractive stimuli, such as AWC (Bargmann et al., 1993), have multiple layers of interneurons interposed (White, 1986).

Male mating is a complex behavior with a partially characterized circuit. Males have about 80 additional neurons, mostly sensory and motor neurons, and mostly in the tail(Sulston et al., 1980). Most of these neurons still have unknown functions. Progress has been made in understanding the set of events that happen during successful mating (Loer and Kenyon, 1993) and some of the neurons that mediate these events (Liu and Sternberg, 1995). For example, the HOB neuron is a sensory neuron required for an initial pause when the tail encounters the hermaphrodite vulva; this neuron expresses TRP channels thought to be involved in sensing the hermaphrodite vulva (Barr et al., 2001; Whittaker and Sternberg, 2004). Next, the PCB and PCC sensory neurons promote probing of the vulva via periodic contraction of the spicules using one calcium channel, and the SPC motor neurons promote sustained protraction, which is caused by activation of a different calcium channel (Garcia et al., 2001). The spicule thus anchors the tail during ejaculation. This circuit offers an opportunity to understand the molecular and

circuit mechanisms for carrying out a series of behaviors in turn, where each step can in theory be informed by the internal state of the circuit as well as by sensory input.

The motor output of the egg-laying circuit has also been characterized. Vulval muscles contract to expel eggs, and both the HSN and VC motor neurons promote egg-laying (although the VC neurons also synapse onto the HSN neurons). Serotonin promotes egg-laying through a EGL-30 (Gαq)-dependent process, released primarily from the HSN motor neuron (Bastiani et al., 2003; Waggoner et al., 1998), which itself is inhibited by serotonin (Shyn et al., 2003). Serotonin promotes release of eggs, but acetylcholine released from HSN and the VCs is likely to initiate egg-laying events (Waggoner et al., 1998). Food strongly promotes egg-laying via unknown circuits; the interneurons and sensory neurons upstream of the motor circuit for egg-laying have yet to be functionally characterized. In addition, mutations in both *goa-1* (Gαo) and *egl-30* (Gαq) have hypothesized effects in the circuit but have yet to be cell specifically rescued.

ASH-mediated avoidance is a relatively simple behavior with a relatively simple circuit (Hart et al., 1995; Maricq et al., 1995). Two simple behavioral building blocks involved in ASH avoidance are the reversal and the omega bend. In a reversal, a worm moving forward reverses briefly before continuing forward in a new direction. The omega turn is a sharp turn in the ventral direction. (on a two-dimensional surface, *C. elegans* crawls on its side, with turns occurring either in the dorsal or ventral direction.) ASH-mediated avoidance behavior is elicited when the nose of the animal encounters one of several noxious stimuli, including osmolarity, nose touch, heavy metals, and bitter compounds

like quinine (Culotti and Russell, 1978; Hilliard et al., 2004; Kaplan and Horvitz, 1993; Sambongi et al., 1999). ASH is glutamatergic; glutamate release by ASH is detected by the GLR-1, GLR-2, and NMR-1 glutamate receptors (Hart et al., 1995; Maricq et al., 1995; Mellem et al., 2002), which are expressed by the command neurons. Thus, in order to cause a reversal, ASH need only activate the reverse command neurons by releasing glutamate, a model consistent with the defects seen in the glutamate receptor mutants.

It is not known for sure which command neurons respond to ASH stimuli; AVB, as well as AVA and AVD, appear to be post-synaptic to ASH (White, 1986). In addition, AVA appears to express at least one inhibitory chloride channel that is activated by glutamate (Mellem et al., 2002). The expression patterns of these chloride channels have not been reported in detail (Dent et al., 1997; Dent et al., 2000), and such a channel in AVB could lead to AVB inhibition by ASH. Cell specific rescue of glutamate receptors could begin to define the circuit better.

Some ASH stimuli appear also to be sensed by sensory neurons in the tail (Hilliard et al., 2002); in these cases, an unknown circuit appears to integrate the two signals to decide whether to move forward or backward. This integration is likely to be carried out by the command neurons, since PHA synapses mostly onto PHB, while PHB (like ASH) synapses onto the command neurons (Hilliard et al., 2002; White, 1986). Being the proposed circuit for multiple sensory integrations (*e.g.*, noxious stimuli and touch) is consistent with a model where the command neurons make a continuous assessment of sensory input from head and tail to decide whether to move forward or backward.

It is not known how ASH stimulates omega turns. ASH synapses onto interneurons involved in multiple navigation behaviors (interneurons shown in Figure 2.3) (White, 1986), and ablation of these interneurons can alter the length of reversals during ASH-mediated avoidance (data not shown). These neurons may also be responsible for omega turns.

One of the most obvious behaviors in *C. elegans* involves the modulation of speed by food. In the N2 strain and other solitary strains, worm locomotion slows dramatically in the presence of bacterial food (Sawin et al., 2000). Slowing on food is mediated by two independent pathways, one involving dopamine and the other regulated by serotonin.

The dopamine pathway is important when well-fed worms encounter food (Sawin et al., 2000). *C. elegans* appears to have only three dopaminergic neuron classes, the single head neuron ADE, the four head CEP neurons, and the PDE neuron in the tail. These neurons act redundantly in this behavior, but without them worms do not slow upon encountering food. Food slowing can be partially reconstituted with a simple physical stimulus, indicating that the dopaminergic cells partly sense touch, although they are likely to sense other elements of food. Dopamine receptors are broadly expressed (data not shown), and it is not known what cells sense the dopamine released by ADE, CEP, and PDE. This circuit could be delineated with cell-specific rescue of dopamine receptors.

The serotonin pathway plays a role when worms have been starved (Sawin et al., 2000). The serotonin is released at least in part from the NSM neuron. What signal NSM responds to is not known, nor is it known which neurons respond to NSM serotonin release. A serotonin receptor channel, MOD-1, is expressed in several interneurons in the navigational circuit (shown in Figure 2.3) and was isolated for failing to slow on food (Ranganathan et al., 2000)(Cori Bargmann, personal communication). Cell specific rescue of this gene should help delineate the circuitry involved in the serotonin component of the response.

Chemotaxis and thermotaxis are two complex behaviors involving worms migrating directionally within gradients of chemicals or temperature (Hedgecock and Russell, 1975; Ward, 1973). These behavioral circuits are not likely to make comparisons between two points in space, since sensory neurons involved are separated only by a few microns (Bargmann et al., 1993; Bargmann and Horvitz, 1991a; Mori and Ohshima, 1995). Instead, the concentration of odor is measured over time. When the environment is improving, worms suppress reversals and omega turns (collectively referred to as pirouettes); when the environment is worsening, reversals and omega turns increase (Pierce-Shimomura et al., 1999; Ryu and Samuel, 2002; Zariwala et al., 2003). Thus, worms chemotaxis much like bacteria (Berg and Brown, 1972), although casual observation suggests that additional mechanisms may also play a role, particularly when stimuli are stronger, such as with higher concentrations of attractants (data not shown).

Circuitry for thermotaxis has been identified using laser ablations, and neurons have been classified depending on whether ablated animals travel toward warmer temperatures (thermophilic), cooler temperatures (cryophilic), or are indifferent (athermotactic)(Mori and Ohshima, 1995). Some interneurons have also been examined for their effects on pirouette frequency during temporal temperature gradients (or ramps) (Ryu and Samuel, 2002; Zariwala et al., 2003).

Circuitry for chemotaxis was analyzed by ablations, but no single ablation abolished the behavior (Cori Bargmann, personal communication), suggesting that the circuit may be distributed. An alternative possibility is that individual elements of chemotactic behavior may be perturbed by individual ablations while other behavioral elements compensate. For example, pirouette output could be compromised while other mechanisms are not.

Oxygen Sensing Pathways

The experiments in Chapter 3 propose a novel oxygen sensor, the soluble guanylate cyclase *gcy-35*. There are several well-established oxygen sensing proteins already, as well as a number of oxygen-sensitive processes with ambiguous or unidentified sensors (Lopez-Barneo et al., 2001). Many channels are regulated by oxygen (Bickler and Donohoe, 2002; Lopez-Barneo et al., 2001), although whether directly or via upstream sensors is often unclear. Two well-established sensors and one recently identified sensor are discussed here.

The hypoxia-inducible factor 1 (HIF-1 in *C. elegans*) transcription pathway, present from nematodes to human beings (Semenza, 2001) is a well-characterized oxygen-sensing pathway. In this pathway, a prolyly hydroxylase, (EGL-9 in *C. elegans*) hydroxylates HIF-1α using oxygen as a substrate. When oxygen is abundant, HIF-1α is hydroxylated, which leads to its ubiquitination and degredation. When oxygen is low (~1%), HIF-1α abundance increases, leading to its binding to HIF-1β and to numerous transcriptional changes, including increased hypoxia viability by upregulating transcripts involved in anaerobic metabolism.

Many gas sensing proteins make use of the heme prosthetic group (Gilles-Gonzalez et al., 1994; Jain and Chan, 2003; Rodgers, 1999), the same heme found in hemoglobin and myoglobin. A well-characterized example is the FixL/FixJ pathway in *Rhizobium*, which regulates the expression of the highly oxygen-sensitive nitrogenase genes involved in nitrogen fixation (Agron et al., 1993; Reyrat et al., 1993; Rodgers, 1999). FixL has a heme-binding PAS domain whose structure has been solved (Gong et al., 1998). In addition to the heme-bound PAS domain, FixL contains a histidine kinase, which is inhibited by oxygen binding to the PAS domain (Monson et al., 1992). Under anaerobic conditions, optimal for nitrogen fixation, FixL is active, phosphorylating itself and then FixJ, a transcription factor. Once phosphorylated, FixJ upregulates nitrogen fixation genes .

The mammalian carotid body represents a case where the sensor is not yet definitively known (Prabhakar, 2005). The carotid body is a millimeter-sized organ located at the main branch of the carotid artery, which feeds the face and brain (Hornbein, 1981). Stimulation of the organ by rising carbon dioxide levels or decreased oxygen results in potent stimulation of breathing (Hornbein, 1981). There are two main cell types in the carotid body, glomus (or type I) cells, which are thought to be the chemoreceptors, as well as support cells (Hornbein, 1981). A recent study (Williams et al., 2004) uses a culture system to identify heme oxygenase-2 as a potential oxygen sensor for the carotid body and potentially many other tissues. Heme oxygenase-2 has traditionally been thought of as a housekeeping enzyme involved in heme degredation (Maines and Gibbs, 2005). However, it turns out that this enzyme can regulate a type of channel implicated in carotid body responses to oxygen (Williams et al., 2004). Glomus cells may be kept in a hyperpolarized state by large conductance, calcium-sensitive BK potassium channels (Nurse and Fearon, 2002). These channels are inhibited by decreases in oxygen, which can depolarize cells. The recent study falls short of proving that heme oxygenase-2 is the carotid body sensor, since knockdown experiments were not performed in carotid body cells.

Chapter 2

A Circuit for Navigation in *C. elegans*

Jesse M. Gray, Joseph J. Hill, and Cornelia I. Bargmann

Abstract

C. elegans explores its environment by interrupting its forward movement with occasional turns and reversals. Turns and reversals occur at stable frequencies but irregular intervals, producing probabilistic exploratory behaviors. Here we dissect the roles of individual sensory neurons, interneurons, and motor neurons in exploratory behaviors under different conditions. After animals are removed from bacterial food, they initiate a local search behavior consisting of reversals and deep omega-shaped turns triggered by AWC olfactory neurons, ASK gustatory neurons, and AIB interneurons. Over the following 30 minutes, the animals disperse as reversals and omega turns are suppressed by ASI gustatory neurons and AIY interneurons. Interneurons and motor neurons downstream of AIB and AIY encode specific aspects of reversal and turn frequency, amplitude, and directionality. SMD motor neurons help encode the steep amplitude of omega turns, RIV motor neurons specify the ventral bias of turns that follow a reversal, and SMB motor neurons set the amplitude of sinusoidal movement. Many of these sensory neurons, interneurons and motor neurons are also implicated in chemotaxis and thermotaxis. Thus this circuit may represent a common substrate for multiple navigation behaviors.

Introduction

As an animal travels through its environment, its nervous system detects sensory cues, evaluates them based on context and the experience of the animal, and converts this information into adaptive movement. For simple behaviors, sensory neurons sometimes communicate directly with motor neurons, but in more complex behavioral circuits, several layers of interneurons integrate sensory information and relay it to motor neurons. The path from sensory input to motor output has been defined in only a few cases, including circuits for crustacean feeding (Nusbaum and Beenhakker, 2002) and circuits for rapid escape in fish, flies, and nematodes (Chalfie et al., 1985; Faber and Korn, 1978; Tanouye and Wyman, 1980). In the nematode *Caenorhabditis elegans,* the escape circuit was defined using a complete synaptic wiring diagram of the 302 neurons in its nervous system (Chalfie et al., 1985; White, 1986). Six mechanosensory neurons that detect noxious stimuli synapse onto four pairs of interneurons called forward and backward command neurons. The command neurons synapse in turn onto motor neurons responsible for forward and backward locomotion, leading to rapid withdrawal from the stimulus. The definition of the escape circuit has enabled analysis of its development, regulation, and modification by experience (Lee et al., 1999; Rankin, 1991; Rankin et al., 2000; Rankin and Wicks, 2000; Wicks et al., 1996; Zheng et al., 1999). The *C. elegans* wiring diagram provides an opportunity to define many complete neuronal paths from sensory stimulus to behavior.

In contrast with the escape circuit, the neuronal control of locomotion during exploratory behavior is poorly characterized. *C. elegans* navigates to favorable conditions by chemotaxis, thermotaxis, and aerotaxis. In these sensory behaviors and in exploratory behaviors in the absence of informative sensory cues, the animal moves forward and occasionally changes its direction of movement either by a transient reversal or by turning its head during forward movement. The largest change in direction is generated in a sharp omega turn during which the animal's body shape resembles the Greek letter (Croll, 1975; Wallace, 1969)(Fig. 1A). Sinusoidal movement itself can also change during navigation, switching between shallow and deep bends. The neuronal pathways that convert sensory information into specific turning behaviors are incompletely defined. The command neurons are not required for the generation of sinusoidal forward movement (Chalfie et al., 1985; Zheng et al., 1999); the neurons that modulate forward movement to cause curving and omega turns are unknown.

In *C. elegans,* taxis behaviors have features of a biased random walk (Pierce-Shimomura et al., 1999; Ryu and Samuel, 2002; Zariwala et al., 2003) (JMG and CIB, unpublished data), a strategy first described in bacterial chemotaxis (Berg and Brown, 1972). During a biased random walk, periods of relatively straight movement ("runs") are occasionally interrupted by periods of rapid direction change ("tumbles" in bacteria and "pirouettes" in *C. elegans*). A pirouette is a period marked by reversals or sharp turns (Pierce-Shimomura et al., 1999). In a biased random walk, individual trajectories are not predictable. However, when the environment is improving (*e.g.,* when concentrations of attractant increase), pirouettes become less frequent. When the environment is declining,

pirouettes become more frequent. This strategy biases the direction of travel toward favorable conditions.

We sought to understand the mechanisms by which sensory neurons modulate the frequency of reversals and turns in *C. elegans*, and the downstream neuronal circuits that generate specific features of these behaviors. The presence of food affects many aspects of *C. elegans* locomotion (de Bono and Bargmann, 1998; Fujiwara et al., 2002; Hills et al., 2004; Sawin et al., 2000). Here we use a systematic analysis of *C. elegans* neuroanatomy to dissect a circuit that uses sensory cues to modulate turning rates in two kinds of exploratory behavior: local search after animals are removed from food, and long-range dispersal after prolonged food deprivation. These exploratory behaviors in the absence of directional cues share many features with a biased random walk. Our results delineate a behavioral circuit for navigation in *C. elegans* from sensory input to motor output.

Materials and Methods

Strains

C. elegans strains were maintained and grown according to standard procedures (Brenner, 1974). The following strains were used: wild-type strain N2, PR811 *osm-6 (p811)* V, PR802 *osm-3 (p802)* IV, CB1033 *che-2 (e1033)* X, CB1112 *cat-2 (e1112)* II, GR1321 *tph-1 (mg280)* II, OH8 *ttx-3 (mg158)* X, CX3299 *lin-15 (n765ts)* X; *kyIs50[odr-*

2b::gfp; lin-15(+)], CX3300 *lin-15 (n765ts)* X; *kyIs51[odr-2b::gfp; lin-15(+)]*, CX6896 *mgIs18[ttx-3::gfp]* IV, *akIs3[nmr-1::gfp] (Brockie et al., 2001).*

Behavioral Assays

Young adult animals were first observed on OP50 food in covered plates for five minutes and then transferred onto a fresh, foodless NGM plate (Brenner, 1974). Observation began one minute after transfer (Zhao et al., 2003). Reversals of three or more head swings were scored as long reversals. Omega turns were visually identified by the head nearly touching the tail or a reorientation of > 135 degrees within a single head swing. Animals were scored by an investigator blind to the genotype or ablation status of the animal.

To score post-reversal turn angles, animals were video-recorded off food and an observer blind to the animal's status drew lines denoting the worm's apparent heading immediately before and immediately after a turn.

A detailed description of behavioral assays appears in Supplementary Methods.

Laser Killing of Neurons

Individual neurons were identified either using Normarski optics and a combination of position and morphological cues (Bargmann and Avery, 1995), or they were identified

using GFP-expressing transgenes. Cells from L1 stage worms were killed using a laser microbeam focused through the 100 x Neofluor objective of a Zeiss Axioskop. Adults were assayed as young adults (not more than 72 hours after the L4 adult molt), which allowed at least 2.5 days following laser surgery for the ablated cells to lose function. Ablated animals were tested with parallel controls of the same genotype (*e.g.*, with the same transgenes, if relevant) on the same day.

Statistical Analysis

Although general features of the behavior patterns were reliable, the specific frequency of reversals or turns could vary from day to day and could be affected by transgenes used for cell identification. Therefore, laser-treated animals were always compared to approximately equal numbers of control animals tested on the same day under the same conditions. Comparisons between tested animals and matched controls were made using Student's t-test (Statview). The results of statistical tests and the sample sizes are available in electronic format upon request.

Results

Reversals and Omega Turns Are Coupled in Pirouettes

C. elegans crawls on its side, flexing in a dorsal-ventral direction to generate sinusoidal movement (Fig. 1A). A turn occurs when the head swings are stronger in either the

ventral or dorsal direction. One large head swing can cause a rapid turn, or a series of gently biased head swings can produce gradual curving. An extreme change of direction of around 180 degrees is generated by the omega turn, also called an omega wave or omega bend (Croll, 1975; Wallace, 1969).

To develop more specific assays for changes in the direction of movement, we categorized different types of reversals and turns by direct observation of freely moving animals. Reversals were scored as any perceptible backward movement of the entire animal, and reversal length was scored according to the number of head swings that took place during the reversal (Fig. 1A). At the end of a reversal, the first forward head swing nearly always incorporated a turn that caused the animal to move forward in a direction different from its initial trajectory (Fig. 1A). A subset of these post-reversal turns were omega turns: sharp turns toward the ventral side of the animal (Croll, 1975). Omega turns were scored according to two criteria: the animal reoriented more than 135 degrees over the course of a single head swing, or the head very nearly approached or touched the tail during the turn (Fig. 1A, panel 4). Although omega turns could occur in isolation, they were often tightly coupled to reversals, such that the animal's head entered the omega turn just as the reversal ended (Fig. 1A, panel 4; Fig. 1B). Omega turns were most commonly coupled to reversals of three or more head swings. In general, the longer the reversal, the more likely it was to end in an omega turns (Fig. 1C). These results are similar to those of Zhao et al (Zhao et al., 2003), who reported that reversals of longer temporal duration were more likely to terminate in omega turns.

The Nature and Frequency of Pirouettes Change in the Absence of Food

To understand how environmental cues regulate the frequency and character of pirouettes, we observed reversals and turns under different conditions. Individual animals were first observed while feeding in solitude. On a lawn of the bacterial food OP50, animals spend most of their time moving forward slowly and reversing frequently, a behavior pattern called dwelling (Fig. 1D) (Fujiwara et al., 2002). We found that reversals in the presence of food were usually short, with only one or two head swings per reversal (Fig. 1E). These short reversals were followed by turns with relatively small turn angles (data not shown). Longer reversals and omega turns were rare on the bacterial lawn.

When animals were transferred to a bacteria-free agar plate, their pattern of locomotion changed dramatically. Immediately after removal from food, the frequency of short reversals declined, and continued to decline for the 40 minutes that the animals were monitored (Fig. 1E). By contrast, the frequency of long reversals (≥3 head swings) increased 10 to 20-fold after removal from food, in parallel with a similar large increase in the frequency of omega turns. Thus, although overall reversal frequencies were similar on food and upon removal from food, the locomotion pattern changed to result in larger changes in direction. In addition, the average speed of forward movement upon removal from food was approximately 10-fold higher than the average speed while on food (data not shown). These changes resulted in rapid exploration of a limited area, a behavior pattern that may represent a local search for food (Fig. 1D)(Hills et al., 2004). At longer times after removal from food, the speed of forward movement remained high,

but the frequency of all reversals and omega turns decreased. As a result, animals moved in long, relatively straight paths, a strategy that may allow them to disperse to distant sources of food (Fig. 1D,E).

These observations define three behavioral states in which the animals move with different patterns of reversals and omega turns: a feeding state on food, which was associated with many short reversals; a local search state shortly after removal from food, which was associated with many long reversals and omega turns; and a dispersal state after prolonged starvation, in which reversals and omega turns were rare. Aspects of these exploratory patterns have also been described by others (Hills et al., 2004; Wakabayashi et al., 2004). For further analysis, we generally studied five-minute time periods representing the local search period (1-6 minutes and 7-12 minutes after removal from food) and the dispersal period after prolonged starvation (35-40 minutes after removal from food), as well as feeding behavior on the bacterial lawn.

Chemosensory Neurons Regulate Exploratory Behavior After Removal from Food

Bacteria present a complex mixture of chemical, mechanical, and nutritional cues to *C. elegans*. To ask whether sensory input contributed to the behavioral changes observed after removal from food, we examined *osm-6* mutants, which are defective in the development of all ciliated chemosensory and mechanosensory neurons (Perkins et al., 1986). On food, *osm-6* mutants exhibited normal feeding behavior, with reversal frequencies and reversal lengths comparable to those of wild-type animals (Fig. 2A).

When removed from food, *osm-6* mutants behaved as though food was still present: they failed to suppress short reversals, and exhibited abnormally low frequencies of long reversals and omega turns (Fig. 2A). After 35 minutes of starvation, *osm-6* mutants continued to execute frequent short reversals, and even several hours of continued starvation did not completely suppress this behavior (data not shown). *che-2* mutants, whose cilia are also defective, exhibited similar behavior (data not shown). These phenotypes suggest that the local search and dispersal behavior patterns are initiated by ciliated sensory neurons, probably those that detect sensory stimuli from food.

osm-6 is expressed in many chemosensory and mechanosensory neurons. To narrow down the list of candidate neurons, we killed the neurons in the amphid chemosensory organs in wild-type animals using a laser microbeam. Like *osm-6* mutants, animals lacking amphid sensory neurons had defects in both local search and dispersal behavior, with reduced suppression of short reversals and little stimulation of long reversals and omega turns (Fig. 2B). An *osm-3* mutation, which inactivates the gustatory but not olfactory neurons (Tabish et al., 1995), had a similar but less severe defect compared to either amphid neuron-ablated or *osm-6* animals (Fig. 2C). These results suggest that both gustatory and olfactory amphid neurons sense environmental changes to trigger local search and dispersal behaviors.

To identify specific cells with a role in local search and dispersal behaviors, individual sensory neurons were killed with a laser microbeam. Three classes of amphid chemosensory neurons had strong effects on the local search and dispersal behaviors.

The two AWC neurons sense volatile olfactory attractants from food to direct chemotaxis (Bargmann et al., 1993). Killing the AWC neurons reduced reversals and omega turns during local search behavior but did not disrupt behavior on food or dispersal behavior (Fig. 2D). A similar effect was observed upon killing the two ASK neurons, which sense water-soluble attractants and repellents (Fig. 2E)(Bargmann and Horvitz, 1991a; Hilliard et al., 2002). These results suggest that AWC and ASK play a role in the local search state by stimulating long reversals and omega turns upon removal from food. By contrast, dispersal behavior required the ASI chemosensory neurons, which also regulate developmental responses to crowding and food deprivation (Fig. 2F). When ASI was killed, short reversals were not suppressed after removal from food, and omega turns were not suppressed at long times off food.

ASI makes several synapses onto AWC (White, 1986), so it seemed possible that ASI might suppress omega turns by inhibiting AWC directly. Animals lacking both ASI and AWC executed fewer short reversals and omega turns than animals lacking only ASI, but turned and reversed more than AWC-ablated animals (Fig. 2F). Thus, ASI-mediated suppression of reversals and omega turns is partly dependent on, and partly independent of, AWC.

No other amphid neuron had effects as substantial as those of AWC, ASK, and ASI. The nociceptive ASH sensory neurons trigger reversals and omega turns in response to many aversive stimuli (Kaplan and Horvitz, 1993), but killing ASH had no effect (Fig. 2G). The two AFD neurons are implicated in thermotaxis (Gomez et al., 2001; Mori and

Ohshima, 1995), and killing AFD led to a small decrease in reversals and omega turns during local search in the first few minutes off food (Fig. 2H). Killing the AWB or ADL sensory neurons that sense volatile repellents, the ASE neurons that sense attractive water-soluble compounds, the AWA neurons that sense attractive odors, or the ASG and ASJ neurons that sense pheromones (Bargmann and Horvitz, 1991b; Schackwitz et al., 1996) had little or no effect (Figs. 2I-N).

The transition from local search to dispersal occurred after starvation. Two secreted neuronal signals that regulate other responses to starvation in *C. elegans* are TGF (*daf-7*), which is produced by ASI neurons (Ren et al., 1996) and serotonin (Sze et al., 2000). The serotonin-deficient mutant *tph-1* was defective in exploratory behavior (Fig. 2O), as was *daf-7* (data not shown), suggesting that these neuronal signaling molecules regulate exploratory behaviors in the absence of food.

A Candidate Circuit for Navigation

To identify interneurons that function in navigation (Fig. 3), we traced the predominant synaptic output of sensory neurons using two approaches (Fig. 3, Supplemental Methods). In the first approach, we identified circuit paths from the amphid sensory neurons to any head motor neurons or command interneurons, focusing on the shortest paths with the most synapses or gap junctions. The command interneurons promote either forward or backward movement; head motor neurons comprise a partially independent motor system that can carry the animal forward even without the forward

command neurons (Chalfie et al., 1985). In the second approach, we followed all synaptic output of the sensory neurons through four layers of downstream synapses, ignoring connections representing only a small fraction of the previous layer's output. This second approach (summarized in Supplementary Table 1) was unbiased with regard to the final output, but the majority of neurons and connections identified were the same as those identified in the first approach.

Four groups of neurons emerged as major direct and indirect targets of the amphid sensory neurons (Fig. 3, Supplementary Table 1, Methods). Half of all synaptic output from the amphid was directed to the interneurons AIA, AIB, AIY, and AIZ (layer 1). These neurons in turn directed a large fraction of their output onto the RIA and RIB interneurons and the head motor neurons RIM and SMB (layer 2). In *C. elegans*, many motor neurons, including RIM and SMB, also synapse onto other neurons. Layer 2 had some synapses onto muscles, but more than half of its output was directed to layer 3, comprised of additional head interneurons and motor neurons (layer 3a: SAA, RIV, RMD, SMD, SIA, and SIB) and the command interneurons (layer 3b). Head motor neurons synapse mostly onto each other and onto muscles in the head.

To test the role of interneurons and motor neurons, we ablated individual neuronal classes and examined spontaneous reversals and omega turns on food and off food during local search and dispersal behaviors. The three interneurons AIZ, AIB, and AIY each had preferential effects on one of the three behavioral states. On food, killing the AIZ neurons resulted in animals with a reduced frequency of short reversals (Fig. 4A). None

of the other interneurons had strong effects on food. The local search behavior after removal from food was strongly affected by killing the AIB interneurons (Fig. 4B). Animals lacking these cells did not exhibit a strong stimulation in long reversals and omega turns upon removal from food. Instead, like AWC or ASK ablated animals, they exhibited premature dispersal behavior, with long runs of forward movement. Dispersal behavior was most strongly affected by killing the AIY interneurons (Fig. 4C). After half an hour off food, animals lacking AIY failed to suppress all classes of reversals and omega turns, instead exhibiting a behavior pattern reminiscent of the local search state.

To further understand the relationships between sensory neurons and interneurons, we examined animals in which multiple classes of neurons were inactivated. Guided by the neuroanatomy in Fig. 3, we assayed several compound lesions. AWC and AIY have opposite effects on reversals and omega turns, and AWC synapses onto AIY, suggesting that AWC might act by directly inhibiting AIY. Indeed, animals lacking both AWC and AIY resembled those lacking only AIY (Fig. 4G).

Both *osm-6* sensory mutants and AIY ablated animals exhibited persistent reversals and turns during the normal period for dispersal. Killing AIY in *osm-6* mutants further increased reversals and turns both on and off food (Fig. 4H), indicating that AIY can suppress reversals and turns even when sensory neurons are defective.

Eliminating AIY (with a *ttx-3* mutation, which also eliminates several other cells) and AIB (by ablation) resulted in an animal distinct from either single manipulation (Fig. 4I):

short reversals were frequent (similar to when AIY was killed), long reversals and omega turns were decreased (as when AIB was killed), and as a result neither local search nor dispersal behavior was normal. Thus, the functions of the AIB and AIY interneurons may be additive, suggesting that these neurons act at least partly in parallel.

The interneurons and motor neurons that receive input from AIB, AIY, and AIZ (Fig. 3) were also analyzed systematically. Their functions were more selective than those of layer 1 interneurons, suggesting a transition from the coordinated regulation of exploratory behaviors (AIB, AIY) to a distributed regulation of smaller sets of behaviors at layer 2. Like animals lacking AIY, animals in which the RIM motor neurons were killed showed an inappropriate persistence of short reversals after removal from food (Fig. 4D); several gap junctions connect AIY and RIM. Like animals lacking AIB, animals in which RIB interneurons were killed had fewer long reversals and omega turns during local search (Fig. 4E); AIB synapses onto RIB. The RIA interneurons had a small effect on long reversals (Fig. 4F). The transition from coordinated control to individual behaviors became more marked in layers 3a and 3b, as described below.

The Navigation Circuit Regulates Reversal Frequency via the AVA Command Neurons and Omega Turns via SMD and RIV Head Motor Neurons

Information from the navigation interneurons can be transmitted to the muscles either through the command neurons and downstream ventral cord motor neurons, or through motor neurons in the head including RMD, SMD, SMB, SIA, SIB, RIM, and RIV

(White, 1986)(Fig. 3). Head neurons belong to symmetrical groups of two (RIM, RIV), four (SMD, SMB, SIA, SIB) or six (RMD) neurons (Fig. 5G legend). Three different sets of muscles are differentially innervated by ventral cord and head motor neurons (Fig. 5G)(White, 1986). The most anterior four rows of muscles, the head muscles, are innervated only by head motor neurons. The next four rows of muscles, the neck muscles, are innervated by head motor neurons and ventral cord motor neurons. The last sixteen rows of muscles are innervated mainly by ventral cord motor neurons, with minor synapses from head motor neurons at the anterior end.

Reversals and backward movement require the backward command neurons AVA and AVD (Chalfie et al., 1985), with minor cross-talk from the forward command neurons AVB and PVC (Zheng et al., 1999). AVA and AVB receive input from the navigation circuit (AIB, RIB, RIM, and SMB) (Fig. 3). Animals lacking the AVA neurons were unable to generate long reversals under any conditions, and generated abnormally few short reversals on food (Fig. 5A). However, omega turns were present at approximately normal frequencies. These results suggest that the navigation circuit stimulates long reversals via the command neuron AVA but can generate short reversals and omega turns using other motor pathways.

Several classes of head motor neurons inhibited reversals. Killing RIM increased the frequency of short reversals; killing both RIM and AVA neurons suppressed the effect of eliminating RIM (Fig. 5A). RIM forms synapses and gap junctions onto the command interneurons, suggesting that it may inhibit short reversals through these connections.

SMB motor neurons also synapse onto the command neurons, and SMB inhibited short reversals to a lesser extent (Fig. 5F). Neither RMD nor SMD synapse directly onto the command neurons, but killing either cell increased the frequency of reversals (Fig. 5B).

Head motor neurons could also affect forward locomotion. Killing the SMB neurons led to a dramatic increase in the amplitude of dorso-ventral head swings, and resulting loopy sinusoidal movement (Fig. 5I). These head bends were so steep that it was not possible to score omega turns accurately when SMB was killed.

Omega turns were stimulated by SMD and RIV motor neurons. Killing SMD led to a small but significant decrease in the frequency of omega turns (Fig. 5B). Because of the concomitant increase in reversal frequency, animals ablated for SMD executed many reversals without omega turns (data not shown). Killing RIV neurons also led to a decrease in the frequency of omega turns. Neither SMD nor RIV was required for reversals, indicating that the final motor pathways for executing reversals (command/ventral cord neurons) and omega turns (SMD, RIV) are largely distinct.

SMD Encodes Omega Turn Amplitude, and RIV Underlies the Ventral Asymmetry of Omega Turns

We next analyzed specific features of the omega turn, a steep asymmetric bend that usually occurs in the ventral direction (Croll, 1975). In intact animals, omega turns occurred with high probability immediately after long reversals (Fig. 1C). In animals in which SMD was killed, long reversals were followed by more shallow turns. The

average angle of post-reversal turns was 137° ± 8° in intact animals, and 72° ±11° in animals in which SMD was killed (Fig. 5H). These results suggest that SMD neurons control the steepness of turning to generate omega turns. RIV motor neurons had a smaller effect on the steepness of turns but a dramatic effect on their ventral bias (Fig. 5H). In intact animals, the first head swing after a reversal was highly biased in the ventral direction, even though not all turns in the ventral direction are omega turns (Fig. 5H). This ventral bias was lost in animals lacking RIV. Killing SMD did not alter the ventral bias (Fig. 5H). These results indicate that RIV biases both omega turns and other post-reversal head swings in the ventral direction.

Among head motor neurons, the RIV motor neuron class is unique in innervating ventral but not dorsal neck muscles (White, 1986). To ask whether the effect of killing RIV could be attributed simply to a generic decrease in ventral muscle innervation in the head, we killed ventral members of several other classes of head motor neurons (SMD, RMD, SMB) while sparing dorsal members. These ablations did not affect the frequency of omega turns, but did in some cases result in gentle curvature of forward movement over the course of several head bends (data not shown).

Discussion

Sensory neurons and interneurons regulate the transition between exploratory behavioral states.

C. elegans has distinct exploratory states in which it changes its overall pattern of locomotion based on its recent experience with food (this work and (Hills et al., 2004; Sawin et al., 2000; Wakabayashi et al., 2004)). The animal's behavior upon removal from food moves from an initial local search state, with many reversals and omega turns, to a subsequent dispersal state with few reversals and omega turns. These two behavioral states require distinct sets of sensory neurons and interneurons (Fig. 5J). The AWC, ASK, and AFD sensory neurons and the AIB and RIB interneurons increase the probability of reversals and turns in the local search state. The ASI sensory neurons and the AIY interneurons decrease the probability of reversals and omega turns and are required for the dispersal state.

In some respects these exploratory behaviors echo the biased random walk, or pirouette, model of chemotaxis. A high frequency of pirouettes is observed after an unfavorable change in the environment (in this case, the disappearance of food). However, in a constant environment, pirouettes eventually decrease to a low baseline level, leading to dispersal. During chemotaxis, the frequency of pirouettes adapts quickly to a change in the stimulus, returning to baseline within a few minutes. By contrast, in exploratory behavior after removal from food the rate of turning falls much more slowly. These results suggest that pirouette rates are regulated by sensory experience across a variety of time scales.

When combined with synaptic connectivity data (White, 1986), the effects of laser ablations on turning frequency can be used to make predictions about the nature of

neurotransmission within the circuit. For example, AWC synapses heavily onto AIY, but these two neurons have opposite effects on turning frequency. A simple hypothesis is that release of neurotransmitter from AWC inhibits AIY activity. Based on this logic, many of the synapses in the navigation circuit may be inhibitory.

The high level of pirouettes during local search behavior reflects a sensory memory of food that is expressed by the navigation circuit. Because ASK and AWC are required for local search, it is possible that the memory of food is partially encoded in the activity of these neurons. The transition from local search to dispersal requires the ASI sensory neurons. Dispersal may be caused by an increase in ASI activity, a decrease in AWC or ASK activity, inputs that have yet to be identified, or some combination of the above. Both serotonin and the TGF-ß molecule DAF-7, which is produced by ASI, contribute to this transition. Serotonin and TGF-ß affect a variety of other neuronal responses associated with starvation (Ren et al., 1996; Sawin et al., 2000).

The AIB interneurons associated with local search and the AIY interneurons associated with dispersal have been identified in several recent papers that examined spontaneous reversal behaviors off food (none of the other studies examined omega turns and different kinds of reversals separately). Wakabayashi et al. (Wakabayashi et al., 2004) described a local search-like behavior shortly after removal from food, which they call pivoting, and a later dispersal behavior, or traveling. Pivoting required AIB interneurons, like local search, and the suppression of reversals in traveling required AIY neurons. AIY also suppresses reversals in other sensory paradigms, and has a smaller role suppressing

reversals during local search and on food (this work, (Ryu and Samuel, 2002; Tsalik and Hobert, 2003; Zariwala et al., 2003)).

Perhaps surprisingly, the sensory neurons identified in different exploratory paradigms were not identical. After removal from food, pivoting requires ASK and AWC sensory neurons, like local search behavior, but is also regulated by AWA and ADL, which did not affect local search (Wakabayashi et al., 2004). A different short-term reversal assay scored between 1 and 4 minutes off food was affected by ASE, AWA and AFD sensory neurons, but not AWC (Tsalik and Hobert, 2003). Long-term traveling behavior was sensitive to ADF, ASH, and AWA sensory neurons, as well as ASI (Wakabayashi et al., 2004), but dispersal required only ASI. Behavior in another assay that compared reversals at short and long times was regulated by dopamine signaling *(cat-2*, which encodes a putative tyrosine hydroxylase*)*, which did not have strong effects in our assays (data not shown)(Hills et al., 2004). We suggest that these differences may be due to the complete set of sensory changes that animals experience when they are removed from food. Our assays in the absence of food were conducted on nematode growth medium (NGM) agar plates, the same plates used for cultivation, whereas others transferred the animals from food to low osmotic-strength assay plates (Hills et al., 2004) or agarose plates that differed from NGM agar in their mechanical properties, pH, and cholesterol content (Wakabayashi et al., 2004). Dopamine mechanosensory signaling is strongly enhanced at low osmotic strength (Schafer et al., 1996), and traveling varies depending on the chemical composition of the assay plate (Wakabayashi et al., 2004). One interpretation of the different results is that animals respond rapidly to changes in food,

chemicals, and osmolarity by regulating reversals and turns; over time, they adapt slowly to all sensory differences between the new condition and their previous condition, leading to a slow transition to the dispersal state. The exact conditions of the assay would define the dominant sensory neurons.

The AIY interneurons have roles in at least four behaviors: dispersal, thermotaxis, regulation of swimming behavior in response to chemical and thermal cues, and behavioral plasticity in paradigms in which starvation is paired with a thermal cue or chemical cue (Ishihara et al., 2002; Mori and Ohshima, 1995; Tsalik and Hobert, 2003). The roles of AIY in thermotaxis and swimming regulation are rapid, and can be explained by direct inputs from sensory neurons onto AIY. However, some of AIY's effects on plasticity could be indirect effects of its general function in suppressing turns and reversals. The frequent reversals in animals lacking AIY could alter locomotion and navigation under many conditions.

Head and Neck Motor Neurons Control Omega Turns and Sinusoidal Movement

The predicted connectivity of *C. elegans* suggests that information from sensory neurons is ultimately directed to head and neck motor neurons that mediate sinusoidal movement and omega turns, and to forward and backward command interneurons. Long reversals are normally tightly coupled to omega turns, but animals lacking the AVA backward command neurons had normal omega turns in the near-complete absence of reversals.

Conversely, SMD and RIV were important in omega turns but were not required for reversals. Thus reversal and omega turn behaviors have distinct final motor pathways.

We found at least four distinct functions for different classes of head motor neurons: regulation of omega turn amplitude (SMD), regulation of omega turn ventral bias (RIV), suppression of short reversals (RIM), and regulation of sinusoidal amplitude (SMB). The RIV motor neurons may provide a ventral bias to omega turns by making synapses only onto ventral muscles; most other head motor neuron classes innervate both ventral and dorsal muscles. The steepest part of the omega bend originates in the neck region (Fig. 1A), where SMD neurons form abundant synapses. Excitatory synapses from SMD to this region may shape the specific properties of the omega turn.

Killing the SMB head motor neurons resulted in high-amplitude sinusoidal movement. This result was surprising, since sinusoidal movement was thought to be generated primarily by body motor neurons. A different kind of loopy behavior, restricted to the head, is observed when RME motor neurons are killed (McIntire et al., 1993). RME forms neuromuscular junctions only onto the most anterior head muscles, whereas SMB innervates head and neck muscles, as well as innervating RME (Fig. 5G). These results suggest that neck muscles can regulate the overall amplitude of sinusoidal forward movement.

Navigation and Probabilistic Behavior

Many features of the navigation circuit remain to be defined. Chief among these is the relationship between this circuit and chemotaxis and thermotaxis behaviors. The sensory neurons involved in chemotaxis and thermotaxis, AWC, AFD, AWA, and ASE, synapse primarily onto the circuit described here, and the interneurons AIY, AIZ, and RIA are required for thermotaxis (Mori and Ohshima, 1995). The regulation of reversals and turns by the circuit described here may play a role in the biased random walk component of taxis.

The well-studied escape behaviors in *C. elegans* are deterministic: a mechanical or chemical repellent leads to a rapid and reliable reversal. By contrast, navigation is probabilistic: it can be described as a set of frequencies, but the exact timing of a particular reversal or turn is unpredictable. Different behavioral states were associated with characteristic frequencies of reversals and omega turns. Most sensory neurons and interneurons regulated the probabilities of several behaviors in a behavioral state. By contrast, motor neurons were more specialized and could even affect individual features of movements. The mechanisms for generating probabilistic behavior are likely to reside in the transformation of information between the sensory neurons, interneurons, and motor neurons in this circuit.

Supplemental Methods

Behavioral Assays

Animals were grown at low density at 20°C. At least one day before assays were performed, each animal was placed on its own agar plate seeded with the bacterial strain OP 50 (Brenner, 1974). Animals were assayed in the first three days of adulthood.

Animals were first observed on food in covered plates for five minutes. If the animal wandered off the food, the assay was aborted and performed again later. Animals were then gently transferred off food with a platinum wire and immediately transferred onto a fresh, foodless NGM plate (Brenner, 1974) that had been air-dried at room temperature for 45-90 minutes prior to the assay. Behavior was scored by direct observation at a Leica M3Z dissecting microscope with the power supply set to 3 V AC. Plates were carefully moved by hand during the assay so that the animal could be observed as it moved across the plate. Observation began one minute after transfer, since the transfer suppresses turning for about one minute (Zhao et al., 2003).

Any backward movement of the entire body was scored as a reversal. Reversal lengths were scored according to the diagram in figure 1A, where reversals of three or more head swings constituted long reversals, and reversals of two or fewer head swings constituted short reversals. This distinction was based on the empirical observation that reversals of three or more head swings occur only rarely on food (Figure 1E). A continuous period of

backward movement was scored as a single reversal. Backward movement that was interrupted by a pause or a brief period of forward movement was scored as two distinct reversals. Omega turns were visually identified by the head nearly touching the tail or a reorientation of > 135 degrees within a single head swing. These criteria were chosen because worms rarely make dorsal turns that match them. For ease of scoring, a UNIX-based Perl script (available upon request) caught keystrokes representing reversals, reversal lengths, and omega turns. During behavioral assays, the script was used in conjunction with Dragon NaturallySpeaking (ScanSoft) voice recognition software for hands-free scoring.

During the experiment, the room temperature was between 20-24°C. Animals that collided with the plastic edge of the plate more than three times during a five-minute assay were discarded. All animals were scored by an investigator blind to the genotype or ablation status of the animal.

To score post-reversal turn angles, animals were video-recorded during the first twelve minutes off food. Angles were measured from the video using two separate frames for each reversal: (1) the frame immediately before the reversal occurred and (2) the frame 1/2 body length after the reversal ended. An observer blind to the animal's status drew lines denoting the worm's apparent heading (in the direction of forward movement) at frames (1) and (2). The reorientation angle was the change between these two frames, where ventral represented positive angles, and dorsal represented negative angles. In the

case of SMD vs. control, only long reversals were considered, since some ablated animals executed frequent short reversals.

Analysis of Circuit Data from White et al., 1986

Digitized data of synaptic connections from two animals (N2U, an adult hermaphrodite; and JSH, an L4 hermaphrodite) (White, 1986) were generated by Richard Durbin and kindly offered online (http://elegans.swmed.edu/parts). Two Perl scripts were created, one to exhaustively find and display point-to-point connections (connect.pl) and another to tabulate connections and compute percentages (tabulate.pl). These are available upon request.

The circuit diagram in Figure 3 was created using three separate approaches, all making use of both N2U and JSH data, although the numbers reported in the figure are those from N2U. For the first approach, circuit paths from the amphid sensory neurons to head and neck motor neurons and to the command interneurons were identified (using connect.pl). Paths with more than two intermediate nodes were discarded, as were paths with small numbers of synapses or gap junctions. Intermediate nodes were arranged in Figure 3 to minimize the length of connecting arrows.

In the second approach, tabulate.pl identified the full complement of neurons downstream of amphid sensory neurons. The most prominent downstream neurons (see below) were classified as layer 1 interneurons. The tablulate.pl analysis was then repeated starting

with the layer 1 interneurons. Three rounds of this analysis generated three layers of downstream neurons. Most of the neurons from this analysis were also identified in the first approach. Layer groupings were intended to simplify the circuit diagram to facilitate understanding, but in some cases the assignments are arbitrary.

Neurons included in each layer (except layer 0, which represented the amphid sensory neurons) passed several inclusion criteria: (1) they represented at least 5% of the previous layer's electrical or chemical synaptic output (assuming number of synapses correlated with strength of connection); (2) they included some input from the major chemotaxis/thermotaxis neurons AWA, AWC, ASE, and AFD (in the case of layer 1) or from multiple neurons in the previous layer (layer 2); (3) they were not more appropriately or conveniently assigned to another layer.

Neurons that matched criterium (1) but were disqualified according to criterium (3) included RIA (excluded from layer 1), AWA and ASI (excluded from layer 2), and RIB (excluded from layer 3). Neurons matching (1) but disqualified according to (2) included ADA, RMG, PVQ, and RIC (excluded from layer 1) and RIG and DVC (excluded from layer 2). AVK and AVE were excluded from layer 3 because they were neither head motor neurons nor command neurons. Head motor neurons URA, IL1, RME, RMF, RMH, and RMG did not match criterium (1) and were not included in Figure 3 or Supplementary Table 1. RMG, the only motor neuron with direct input from amphid sensory neurons, received synapses only from sensory neurons implicated in avoidance responses (AWB, ADL, ASK, and ASH).

In the third approach, inputs to head and neck motor neurons were examined to identify neurons that made a different number of connections to the dorsal and ventral members of a single motor neuron class (e.g. RMD dorsal vs. RMD ventral). This analysis identified one additional neuron class, RIV, as well as neurons identified from the first two approaches.

Acknowledgements

We thank Villu Maricq, Ikue Mori, and Jon Pierce-Shimomura for comments on the manuscript; Shawn Lockery, Thomas Hills, Sreekanth Chalasani, and Tim Yu for valuable discussions; and Takeshi Ishihara and the *Caenorhabditis* Genetics Center (CGC) for strains. This work was supported by funding from the Howard Hughes Medical Institute. J.M.G was supported by a Howard Hughes Medical Institute Predoctoral Fellowship, and C.I.B. is an Investigator of the Howard Hughes Medical Institute.

Figure legends

Figure 1. Regulation of Reversals and Omega Turns During Feeding, Local Search, and Dispersal.

A. Four different examples of reversals of different lengths and degrees of reorientation. Tracks are visible as indentations in the agar. r1, reversal with a single head swing followed by a ~40° change in direction; r2, reversal with two head swings and a ~70° change in direction; R3, reversal with three head swings and a ~90° change in direction; R4, reversal with four head swings followed by an omega turn, resulting in a ~170° change in direction. Blue dots indicate position of the animal's head at the start of the reversal. Anterior is up. In the rightmost panel, D indicates the dorsal side and V the ventral side of the animal during the omega turn.

B. Some omega turns occur in the absence of a reversal, but most occur after a reversal. Most omega turns occur after a reversal of length R3+ (three head swings or greater). N= 285 omega turns. Animals were scored at 1-12 minutes off food.

C. The longer a reversal, the more likely it is to terminate in an omega turn. N= 249 omega turns. Animals were scored at 1-12 minutes off food.

D. Tracks of individual animals feeding on food, in the local search period during the first 12 minutes off food, and during dispersal after 40 minutes off food. The time intervals shown represent about 10 minutes, five minutes, and 30 seconds, respectively.

E. Frequency of short reversals (r1, r2), long reversals (≥R3), and omega turns during 5-minute intervals on food and at different intervals off food.

Figure 2. Sensory Regulation of Local Search and Dispersal Behaviors.

A. *osm-6 (p811)* mutants exhibit dwelling-like behavior (feeding behavior) in the absence of food, with more short reversals and fewer long reversals than controls.

B. Animals with all amphid neurons killed have abnormal local search and dispersal behaviors.

C. *osm-3 (p802)* mutants exhibit milder defects in the absence of food.

D.,E. Killing the AWC or ASK neurons blunts local search behavior, with fewer long reversals and omega turns at 1-6 and 7-12 minutes.

F. Killing ASI disrupts dispersal behavior. Killing ASI and AWC gives a mixed defect.

G.-N. Killing ASH, AFD, AWB, ADL, ASJ, AWA, ASE, or ASG sensory neurons has minor effects or no effect on feeding, local search, and dispersal behaviors.

O. *tph-1 (mg280)* mutants exhibit dwelling-like behavior off food, as indicated by higher frequency of short reversals.

For Figures 2,4 and 5, the "food" column refers to a five minute interval on food, and the other columns refer to intervals after removal from food. The 1-6 and 7-12 minute intervals correspond to the local search state, and the 35-40 minute interval corresponds to dispersal. Short reversals, r1 or r2; long reversals, ≥R3 (see Fig. 1). For each data point, the circle size indicates the frequency of the behavior. Gray circles indicate controls or values not significantly different from controls. Colored circles denote statistical significance; blue circles indicate increases from control values and red circles indicate decreases. The absence of a symbol indicates a value between 0 and 0.05; a red

zero indicates a value in the same range that is statistically different from the control. nd = not done.

Figure 3. A Predicted Circuit for Navigation

A. Data from serial section reconstructions of electron micrographs (White, 1986) were used to assemble a circuit, as described in Supplementary Methods. Each of the following neurons represents a bilaterally symmetric left-right pair: AWC, ASI, ASK, AIY, AIZ, AIB, AIA, RIA, RIM, RIB, RIV. The head and neck motor neurons RMD, SMD, SIA, SMB, and SIB each have four members that innervate muscle quadrants (see Fig. 5). The interneuron SAA also has four members, a ventral and dorsal member on each side. RMD is a class of six radially arrayed neurons. Red dotted lines indicate connections that were asymmetric in the dorso-ventral direction (*e.g.*, 7 of 8 synapses from AIB to SMD are to the dorsal SMDs). The command interneurons are indicated in green.

B. A schematic showing information flow from sensory neurons to motor neurons.

Figure 4. Interneurons Regulate Pirouette Frequency

A. Killing AIZ reduces reversals during feeding.

B. Killing AIB disrupts local search behavior.

C. Killing AIY disrupts dispersal behavior.

D. Killing RIM increases short reversals during feeding, local search, and dispersal.

E. Killing RIB reduces reversals during local search.

F. Killing RIA slightly decreases reversals during local search and dispersal.

G. AWC-AIY double ablated animals resemble AIY-ablated animals.

H. Killing AIY in an *osm-6 (p811)* background increases reversals and turns.

I. Killing AIB in a *ttx-3 (mg280)* background reduces reversals and turns.

Figure 5. Motor Neurons and the AVA Command Neuron have Discrete Functions in Reversals, Omega Turns and Sinusoidal Movement.

A. Killing AVA eliminates long reversals in local search and diminishes short reversals during dwelling. Killing both RIM and AVA results in fewer reversals than an RIM ablation alone.

B. Killing SMD reduces the frequency of omega turns. Killing either SMD or RMD increases reversal frequency.

C. Killing RIV reduces the frequency of omega turns.

D., E. Killing SIA or SIB does not affect omega turns.

F. Killing SMB increases short reversal frequency. ~ indicates that because of loopy movement, omega turns could not be accurately scored.

G. Anatomy of head and neck motor neurons and muscles. Left, innervation of the first ten muscle rows, and approximate position of the muscle rows with respect to the pharynx (gray). Muscle groups are symmetric on the left and right sides; in this schematic only dorsal left and ventral left muscles are shown. SIA and SIB were originally identified as interneurons, but also have neuromuscular junctions (David Hall, personal communication). IL1, URA, RMF, RMG, and RMH motor neurons are not shown. Right, the four muscle quadrants: dorsal-left (DL), dorsal-right (DR), ventral-left (VL), and ventral-right (VR), and the location of head motor neuron synapses onto the muscles in the nerve ring.

H. Killing SMD reduces the amplitude of turns after a reversal, and killing RIV eliminates the ventral bias of post-reversal turns. Turns were scored immediately after a reversal (Fig. 1A). Green arrows and numbers indicate the average angle by which the direction of movement changed after the turn. A ventral turn was scored as positive (0-180°)(blue dots), and a dorsal turn as negative (0-180°)(red dots). Black arrows and numbers indicate the average absolute angle by which the direction of movement changed after the turn. For this analysis, both ventral and dorsal turns were scored as positive (0-180°). Sample sizes are 30, 27, 41, and 68 for control (SMD), SMD, control (RIV), and RIV (at least three worms each). t-test comparisons indicate statistical significance at $p < 0.02$ for SMD vs. control and RIV vs. control, comparing either the averages or the averages of the absolute values.

I. Killing SMB results in deeply flexed, loopy sinusoidal movement. Movement tracks are visible on the agar.

J. Neuronal functions in the navigation circuit from sensory input to motor output. ASI may act partly by inhibiting AWC. ASK and AWC may act by inhibiting AIY and stimulating AIB. Omega turns are generated by head motor neurons, and reversals by the command interneurons.

Supplementary Table 1. Predicted Navigational Circuit Connectivity. Data are averaged across the N2U and JSH worms from White et al, 1986. In each column, percentages represent the percent of connections that neurons in one row make up out of the total connections to neurons in all rows. For example, amphid neurons (layer 0) receive 13% of their synaptic input from layer 1, while layer 1 sends 11% of its synaptic

output to layer 0. The "Receive" column describes connections for which the layer listed at top is postsynaptic. The "Send" column describes connections for which the layer at top is presynaptic. Gap jxn refers to gap junctions. Columns do not always add up to 100% due to effects of rounding. Layer 0 contains the twelve amphid sensory neurons (AWC, AWB, AWA, ASI, ASG, ADL, ADF, AFD, ASH, ASE, ASJ, and ASK). Layer 1 contains the interneurons AIA, AIB, AIY, and AIZ. Layer 2 contains the interneurons RIA and RIB and the head motor neurons RIM and SMB. Layer 3a contains the head motor neurons RIV, RMD, SMD, SIA, SIB, and the interneurons SAA. Layer 3b contains the command neurons AVA, AVB, AVD, and PVC. Inclusion criteria were the same as for Figure 3.

Figure 2.1

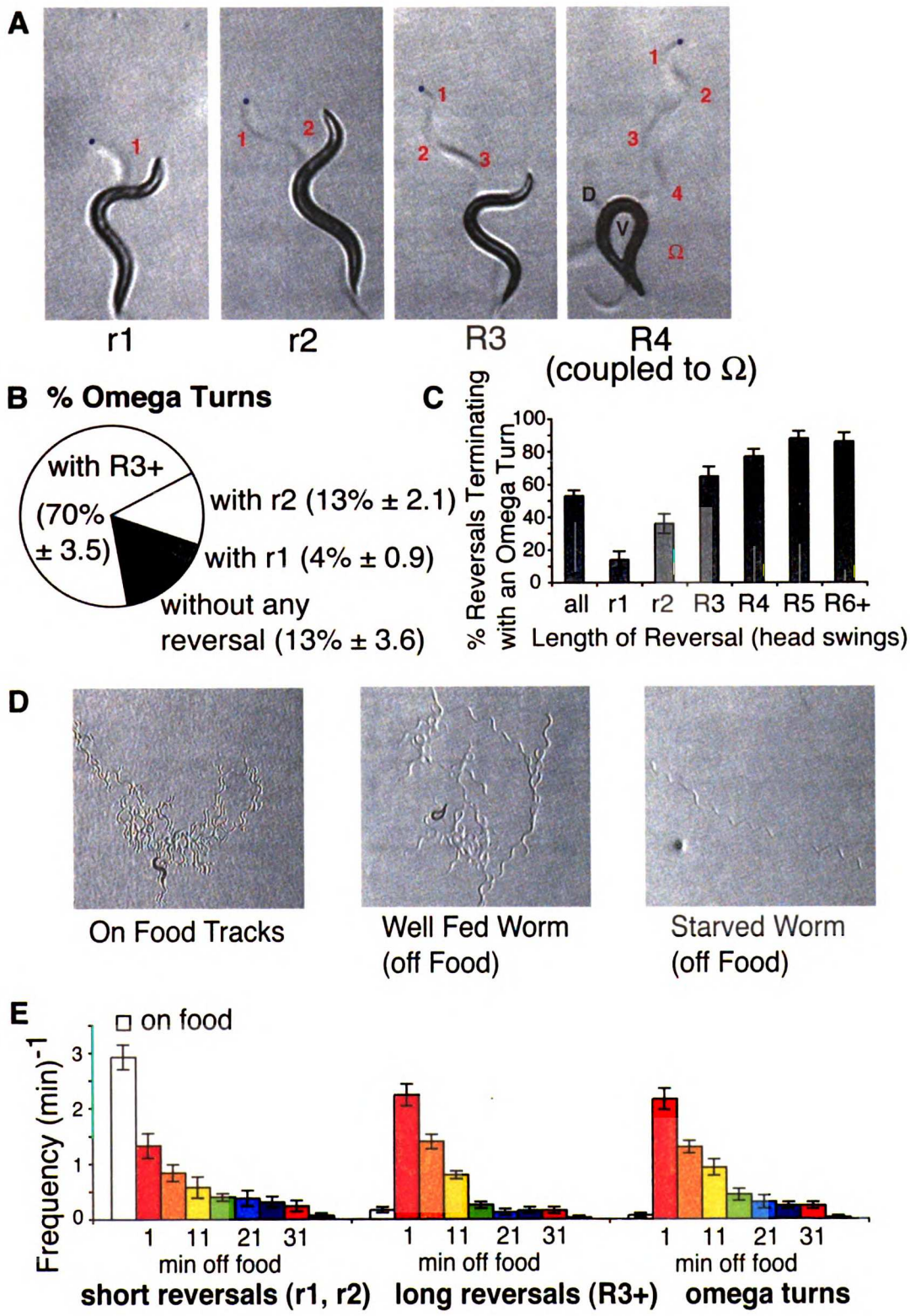
A
r1
r2
R3
R4
(coupled to Ω)
B % Omega Turns
with R3+
(70%
± 3.5)
with r2 (13% ± 2.1)
with r1 (4% ± 0.9)
without any
reversal (13% ± 3.6)
C
% Reversals Terminating
with an Omega Turn
all r1 r2 R3 R4 R5 R6+
Length of Reversal (head swings)
D
On Food Tracks
Well Fed Worm
(off Food)
Starved Worm
(off Food)
E
on food
Frequency (min)-1
min off food
short reversals (r1, r2)
long reversals (R3+)
omega turns

Figure 2.2

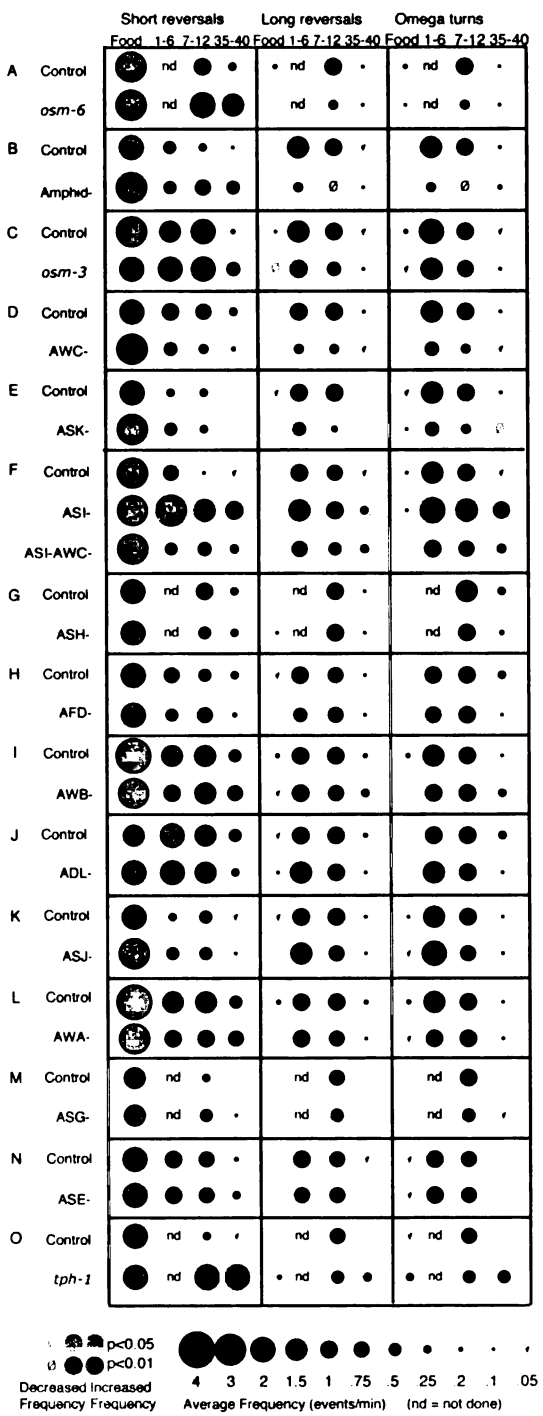

Figure 2.3

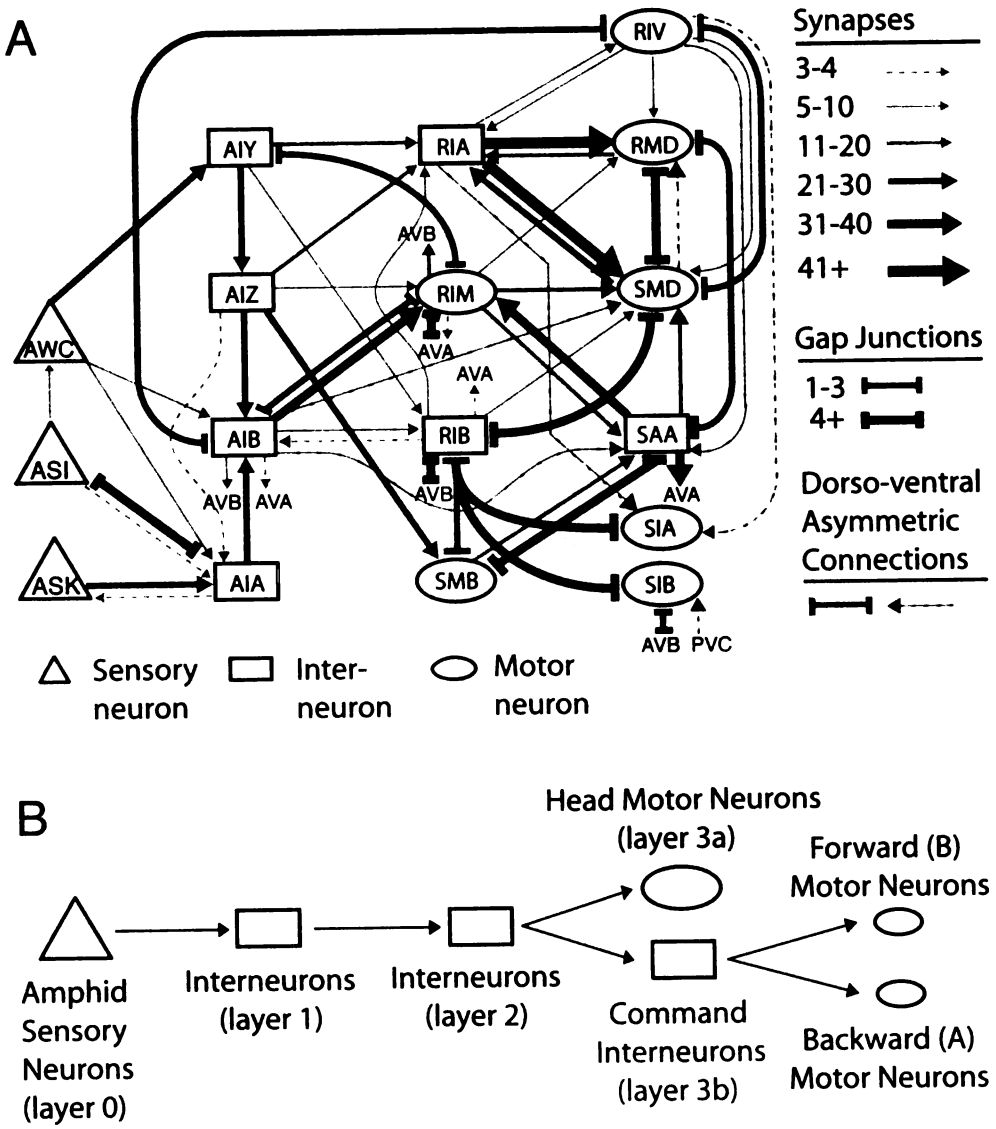

Figure 2.4

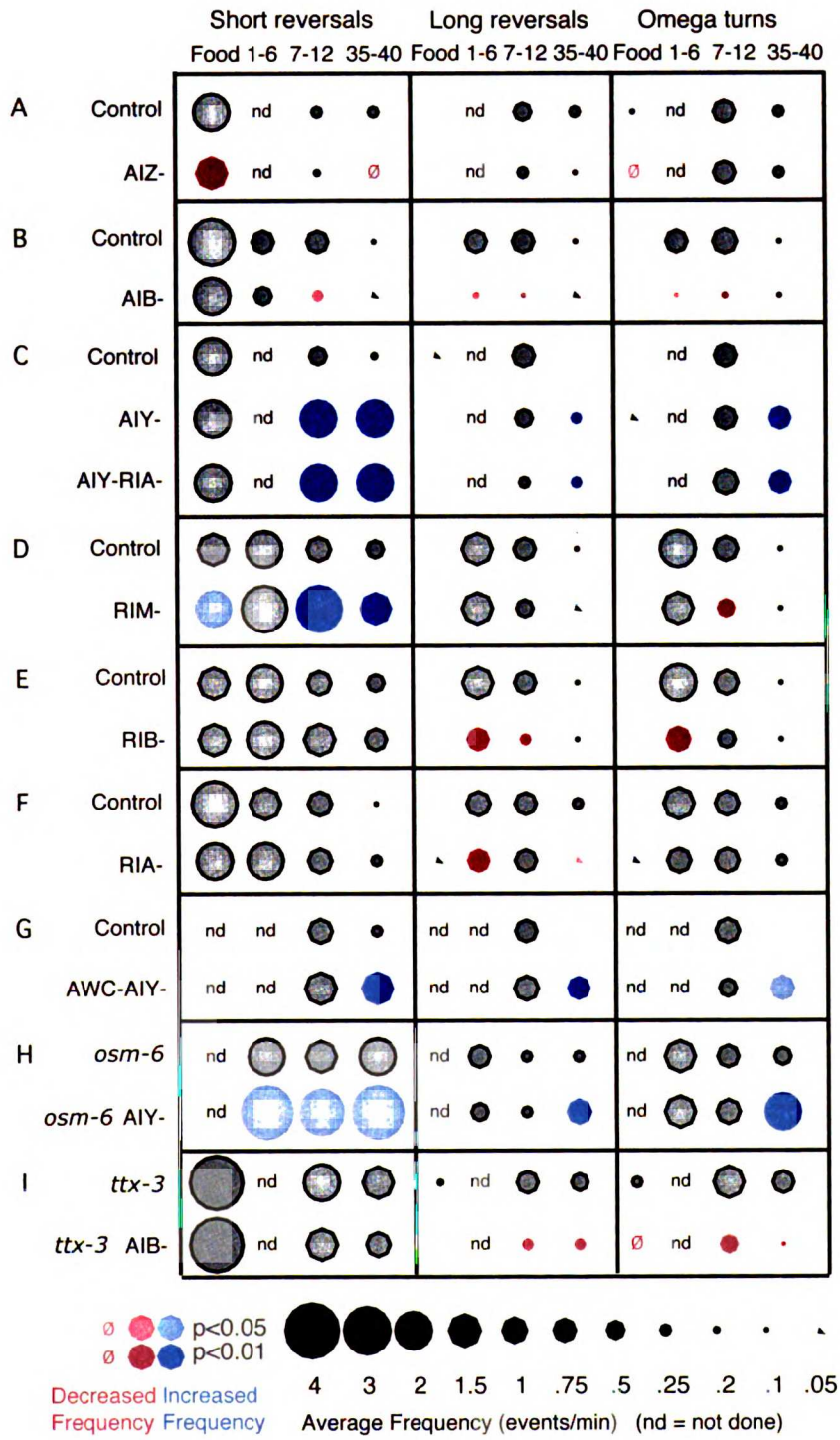

Figure 2.5

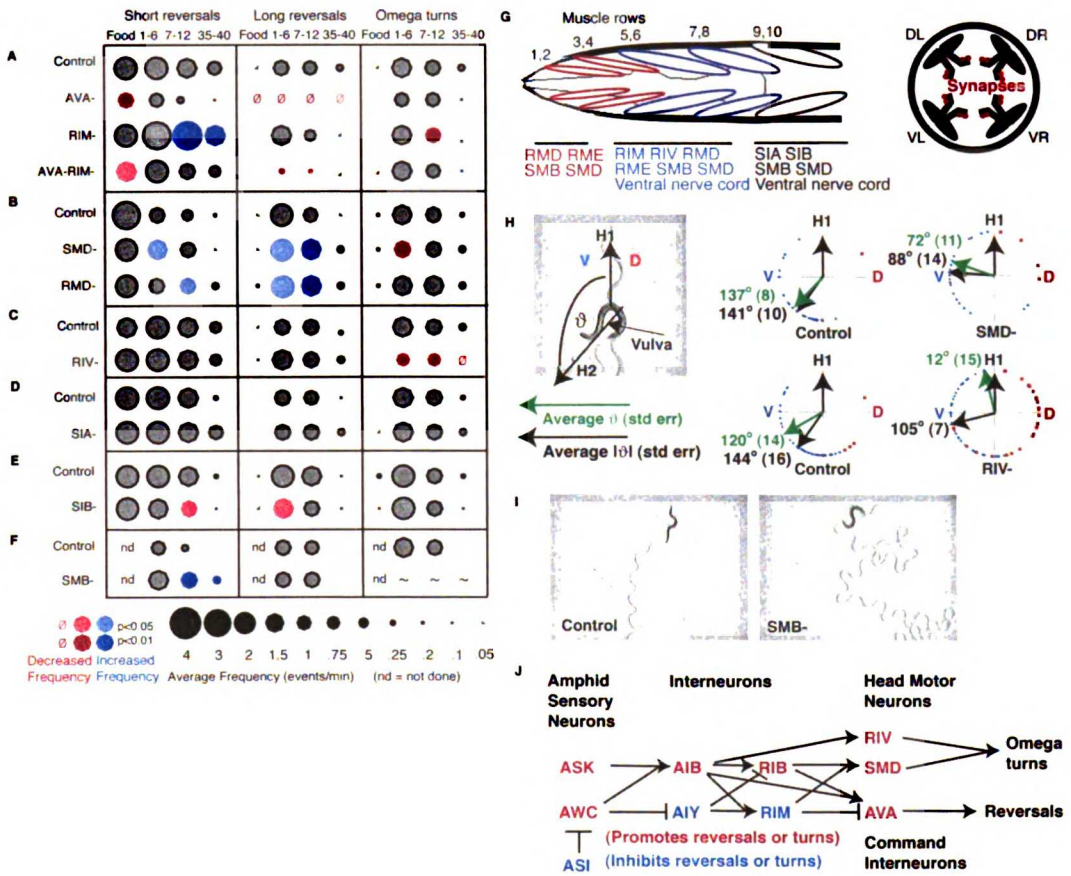
Short reversals
Long reversals
Omega turns
Food 1-6 7-12 35-40
A Control
AVA-
RIM-
AVA-RIM-
B Control
SMD-
RMD-
C Control
RIV-
D Control
SIA-
E Control
SIB-
F Control
SMB-
nd
p<0.05
p<0.01
Decreased Frequency
Increased Frequency
4 3 2 1.5 1 .75 .5 .25 .2 .1 .05
Average Frequency (events/min)
(nd = not done)
G
Muscle rows
1,2 3,4 5,6 7,8 9,10
DL DR
Synapses
VL VR
RMD RME
SMB SMD
RIM RIV RMD
RME SMB SMD
Ventral nerve cord
SIA SIB
SMB SMD
Ventral nerve cord
H
H1
V
D
Vulva
H2
Average ϑ (std err)
Average |ϑ| (std err)
137° (8)
141° (10)
Control
72° (11)
88° (14)
SMD-
120° (14)
144° (16)
Control
12° (15)
105° (7)
RIV-
I
Control
SMB-
J
Amphid Sensory Neurons
Interneurons
Head Motor Neurons
ASK
AWC
ASI
AIB
AIY
RIB
RIM
RIV
SMD
AVA
Omega turns
Reversals
(Promotes reversals or turns)
(Inhibits reversals or turns)
Command Interneurons

Supplementary Table 2.1

	Amphid			AWC,AFD,ASE			AIA,AIB,AIY,AIZ		
	Receive	Gap	Send	Receive	Gap	Send	Receive	Gap	Send
Amphid Sensory	56%	28%	20%	66%	43%	20%	63%	35%	11%
AIA AIB AIY AIZ	13%	26%	50%	18%	57%	76%	16%	20%	29%
RIA RIB RIM SMB	0%	0%	10%	0%	0%	2%	3%	6%	41%
Head Motor Neurons	0%	0%	0%	0%	0%	0%	0%	3%	5%
Command Interneurons	0%	1%	8%	0%	0%	0%	0%	0%	4%
Other	30%	46%	13%	16%	0%	1%	18%	37%	10%
(Total Connections)	222	98	624	103	7	172	491	72	277

	RIA,RIB,RIM,SMB			Head MN			Command		
	Receive	Gap	Send	Receive	Gap	Send	Receive	Gap	Send
Amphid Sensory	11%	0%	0%	0%	0%	0%	10%	1%	0%
AIA AIB AIY AIZ	21%	4%	3%	2%	1%	0%	2%	0%	0%
RIA RIB RIM SMB	4%	14%	5%	38%	25%	30%	5%	24%	0%
Head Motor Neurons	18%	34%	63%	14%	52%	29%	7%	4%	5%
Command Interneurons	0%	15%	6%	0%	2%	11%	9%	20%	66%
Muscles	0%	0%	9%	0%	0%	23%	0%	0%	0%
Other	46%	33%	13%	45%	20%	6%	66%	52%	29%
(Total Connections)	536	112	418	701	156	326	493	72	69

Chapter 3

Oxygen Sensation and Social Feeding Mediated by a C. elegans Guanylate Cyclase Homolog

Jesse M. Gray and David S. Karow (co-first authors), Hang Lu, Andy J. Chang, Jennifer S. Chang, Ronald E. Ellis, Michael A. Marletta, and Cornelia I. Bargmann

Introduction

Specialised oxygen-sensing cells in the nervous system generate rapid behavioural responses to oxygen. We show here that the nematode *Caenorhabditis elegans* exhibits a strong behavioural preference for 5-12% oxygen, avoiding higher and lower oxygen levels. cGMP is a common second messenger in sensory transduction and is implicated in oxygen sensation. Avoidance of high oxygen by *C. elegans* requires the sensory cGMP-gated channel *tax-2/tax-4* and a specific soluble guanylate cyclase homolog, *gcy-35*. The GCY-35 haem domain binds molecular oxygen, unlike the haem domains of classical NO-regulated guanylate cyclases. GCY-35 and TAX-4 mediate oxygen sensation in four sensory neurons that control a naturally polymorphic social feeding behaviour in *C. elegans*. Social feeding and related behaviours occur only when oxygen exceeds *C. elegans*' preferred level, and require *gcy-35* activity. Our results suggest that GCY-35 is regulated by molecular oxygen, and that social feeding can be a behavioural strategy for responding to hyperoxic environments.

All animals require oxygen as the essential electron acceptor in respiration and respond to oxygen levels with behavioural and physiological changes. Soil, fresh-water, and marine

animals encounter and avoid steep oxygen gradients in their natural environments(Wu, 2002)·(Wannamaker and Rice, 2000)·(Sylvia, 1998). In mammals, oxygen acts through the hypoxia-inducible transcription factor HIF-1 to regulate erythropoietin production, red blood cell development, angiogenesis, and cardiovascular physiology(Semenza, 2000). However, behavioural responses to oxygen occur much more rapidly than can be explained by changes in transcription. For example, the mammalian carotid body regulates ventilatory and circulatory responses to hypoxia within seconds(Lopez-Barneo, 2003). The molecular nature of rapid oxygen sensation in the nervous system is not well-understood.

Results

GCY-35 Mediates Oxygen Sensation

An aerotaxis assay was developed to examine oxygen-related behaviours in the nematode *C. elegans*. Washed wild-type animals were placed in a gas-phase oxygen gradient from 0-21% produced by diffusion in a microdevice made in poly(dimethylsiloxane) (PDMS)(Duffy et al., 1998) and allowed to move freely on an agar surface (Fig. 1a,b). Animals distributed across the surface avoiding low oxygen concentrations (<2%) as well as high oxygen concentrations (>12%) (Fig. 1c). The avoidance of hypoxia is consistent with previous studies(Dusenbery, 1980), whereas avoidance of hyperoxia has not been described.

cGMP has been implicated in oxygen responses in *Drosophila*, where a nitric oxide-sensitive, cGMP-dependent kinase pathway mediates behavioural avoidance of

hypoxia(Wingrove and O'Farrell, 1999). In cGMP second messenger cascades, cGMP is produced from GTP by either membrane-bound guanylate cyclases or soluble guanylate cyclases (sGCs). All active sGCs characterised to date contain a haem cofactor and are activated by nitric oxide (NO), which is produced by NO synthase. Notably, however, other hemoproteins can bind oxygen, and prokaryotic hemoproteins mediate aerotaxis to preferred oxygen concentrations(Hou et al., 2000; Jain and Chan, 2003). The genome of the nematode *C. elegans* contains seven predicted sGC homologues (*gcy-31* through *gcy-37*) but no predicted NO synthase, suggesting that these cyclases might detect ligands other than endogenously-produced NO(Yu et al., 1997)·(Morton et al., 1999). The GCYs have the conserved histidine that ligates heme in mammalian β subunits (Suppl. Fig 1)(Morton, 2004b), and conservation of key catalytic residues from both α and β mammalian subunits suggests that *C. elegans* GCYs could be catalytically active (Suppl. Fig 1)(Morton, 2004b). These genes were examined in more detail to determine whether they play a role in *C. elegans* oxygen sensing.

Previous studies demonstrated that *gcy-32* is expressed in URX, AQR, and PQR sensory neurons and that *gcy-33* is expressed in BAG sensory neurons(Yu et al., 1997). The expression patterns of *gcy-34, gcy-35, gcy-36,* and *gcy-37* were examined in transgenic animals bearing reporter genes in which upstream sequences for each gene were fused to sequences encoding the green fluorescent protein (GFP). Each transgene was expressed in a small number of neurons (Fig. 2 and data not shown). Expression of *gcy-34, gcy-35, gcy-36,* and *gcy-37* was consistently observed in URX, AQR, and PQR sensory neurons; *gcy-35* expression was also observed in ALN, SDQ, and BDU neurons and variably in AVM, PLM and PLN neurons, pharyngeal and body wall muscles, and

the excretory cell. The cells that reliably express *gcy-31-gcy-37* have the morphology of sensory neurons, suggesting a sensory role of the GCY proteins, but the sensory cues that activate these cells are unknown.

A *gcy-35(ok769)* mutant from the *C. elegans* knockout consortium was characterised in the aerotaxis assay. *gcy-35(ok769)* deletes sequences corresponding to amino acids 456-545 of GCY-35, including key residues in the GC catalytic domain (Suppl. Fig. 1), and should abolish any ability of the *gcy-35(ok769)* gene product to produce cGMP. In striking contrast to wild-type animals, *gcy-35(ok769)* animals avoided hypoxia but not hyperoxia in gas-phase oxygen gradients (Fig. 1d, Suppl. Fig. 2). This defect did not appear to be due to a general locomotory deficit, as *gcy-35* animals were mobile and chemotaxis-proficient (data not shown). The aerotaxis defect was rescued by expression of a *gcy-35* cDNA in URX, AQR, and PQR (Fig. 1d, Suppl. Figs. 2,3). Thus *gcy-35* can act in URX, AQR, and PQR sensory neurons to mediate avoidance of hyperoxic conditions.

cGMP can depolarise neurons by activating cyclic nucleotide-gated channels(Finn et al., 1996). A cGMP-gated sensory transduction channel in *C. elegans* is composed of two subunits encoded by the *tax-2* and *tax-4* genes, which are co-expressed with *gcy-35* in URX, AQR, and PQR neurons(Coburn and Bargmann, 1996; Komatsu et al., 1996). To ask whether GCY-35 might act upstream of the cyclic nucleotide-gated channel, *tax-4* and *tax-2* mutant and *tax-2; tax-4* double mutant strains were tested for aerotaxis behaviours. Like the *gcy-35* strain, *tax-4* and *tax-2* mutants failed to avoid hyperoxic conditions (Fig. 1e; Suppl. Fig. 2,3). The *tax-4* mutant defect was rescued by expression

of *tax-4* in AQR, PQR, and URX (Suppl. Figs. 2,3). These results indicate that the cGMP-gated channel is required for avoidance of hyperoxia, perhaps as the target for cGMP produced by GCY-35. In support of this model, a *tax-4; gcy-35* double mutant exhibited an aerotaxis defect resembling that of single mutants (Suppl. Figs. 2,3).

GCY-35 Haem Domain Binds Molecular Oxygen

Gaseous ligands bind to sGCs through associated haem groups. To investigate the potential ligand-binding characteristics of GCY-35, we cloned, expressed, and purified the N-terminal predicted haem-binding fragment GCY-35(1-252). This protein was soluble (unlike full-length GCY-35) and tractable for biochemical analysis. Previous studies have shown that N-terminal haem-binding regions of the rat sGC β1 subunit, β1(1-385) and β1(1-194), are spectroscopically similar to the full-length enzymes (data not shown and (Zhao and Marletta, 1997)). Therefore, the GCY-35(1-252) haem domain spectrum should be related to the ligand-binding characteristics of the full-length protein.

GCY-35(1-252) was characterised by UV/visible spectroscopic analysis in the absence and presence of bound ligands. In an anaerobic environment, the purified protein was chemically treated with ferricyanide and dithionite to remove any ligands and to reduce the haem iron to its ferrous oxidation state. The Fe^{+2}-unligated, anaerobic spectrum of this protein exhibited a Soret maximum of 430 nm and a single, broad α/β region that was similar to ferrous-unligated sGC (Fig. 3a,c).

To test for oxygen binding, the unligated protein was exposed to air and immediately reanalysed by UV/vis spectroscopy. The resulting spectrum was

characteristic of oxygen-bound haem, exhibiting a Soret maximum of 415 nm and a split α/β region similar to ferrous-oxy haemoglobin, indicative of a ferrous, low-spin complex (Fig. 3a,c). Like haemoglobin, GCY-35(1-252) was also able to bind NO and CO (Fig. 3c). In the presence of NO, GCY-35(1-252) exhibited a Soret maximum of 415 similar to that of haemoglobin and a shoulder at 400 nm similar to the Soret maximum of NO-bound sGC, suggesting that GCY-35(1-252) forms two stable nitrosyl complexes: a 5-coordinate high-spin complex that is similar to sGC and a 6-coordinate, low-spin complex that is similar to haemoglobin. The ligand-binding characteristics of the GCY-35 haem domain were most similar to oxygen-binding proteins like haemoglobin, and suggest that this protein could act as an oxygen sensor. No other native sGCs or sGC haem domain fragments characterised to date have been found to bind O_2. GCY-35(1-252) is unique in this respect.

Oxygen Regulates Social Feeding Behaviour

The URX, AQR, and PQR neurons that co-express *gcy-35* and *tax-4* have previously been implicated in cGMP-mediated behaviours. The cyclic nucleotide-gated channel TAX-4 is required in these neurons to promote social feeding, or aggregation on a bacterial lawn, and bordering, the accumulation of animals on the thickest part of a bacterial lawn(Coates and de Bono, 2002). Aggregation, bordering, burrowing into agar, and hyperactive locomotion represent a cluster of related behaviours that are not pronounced in the standard *C. elegans* laboratory strain, N2. However, social feeding behaviours are prominent in naturally isolated *C. elegans* strains that differ from N2 at the *npr-1* locus and in N2 strains that are deficient for the function of *npr-1*(de Bono and Bargmann, 1998). *npr-1* encodes a G protein-coupled receptor for FMRFamide-like

neuropeptides, and high levels of *npr-1* activity suppress aggregation and bordering behaviours(Rogers et al., 2003). *tax-4* cGMP signaling stimulates aggregation and bordering by activating the URX, AQR, and PQR neurons (as well as other neurons), whereas *npr-1* functions in URX, AQR, and PQR to inhibit aggregation and bordering(Coates and de Bono, 2002). These reciprocal results suggest that the activity of URX, AQR, and PQR regulates aggregation and bordering behaviours.

If the GCYs expressed in URX, AQR, and PQR are molecular oxygen sensors, then oxygen should regulate the activity of these cells. To test this hypothesis, aggregation and bordering behaviours were examined in animals exposed to a constant flow of gas with different concentrations of oxygen. Initial experiments were conducted by shifting animals from 21% to 7% oxygen, the concentration that was preferred by *C. elegans* in aerotaxis experiments. *npr-1(ad609)* is an EMS-induced loss-of-function mutation, and *npr-1(g320)* is the reduced-function allele of *npr-1* present in natural social strains(de Bono and Bargmann, 1998). *npr-1(ad609)* mutants shifted to 7% oxygen rapidly suppressed both aggregation and bordering behaviours (Fig. 4b,d,f). Suppression was evident within three minutes of shifting to 7% oxygen and was stable for at least thirty minutes following the shift (Fig. 4d,f). A return to 21% oxygen led to the reappearance of aggregation and bordering behaviours within three minutes (Fig. 4d,f). Similar effects were seen with *npr-1(g320)* (data not shown).

A smaller shift from 21% oxygen to 15% oxygen or 10% oxygen led to a similar, but less marked suppression of aggregation and bordering behaviours (Fig. 5a,b). In all cases, the change in behaviour was reversed by returning to 21% oxygen. Thus decreases

in oxygen lead to a dose-dependent suppression of social feeding behaviour, suggesting that oxygen serves as a quantitative regulator of social feeding by URX, AQR, and PQR.

Bacteria Alter Oxygen Levels and Responses

All behaviours in the social feeding cluster are most pronounced in the presence of bacterial food(de Bono and Bargmann, 1998). The aerotaxis assay is conducted in the absence of food, and under these circumstances *npr-1* strains exhibited aerotaxis with preferred concentrations similar to those preferred by N2 animals (Fig. 1f). Because social behaviours are food-induced, we also tested aerotaxis in N2 and *npr-1* strains in the presence of food (Fig. 5c, Suppl. Fig. 2). On a thin bacterial lawn, aerotaxis behaviours in N2 were blunted, with a greatly reduced avoidance of hyperoxia. By contrast, *npr-1* strains exhibited robust hyperoxia avoidance in the presence or absence of food.

How does oxygen sensation relate to the cluster of social feeding behaviours? We observed that the thick lawns of *E. coli* that are usually fed to *C. elegans* consume oxygen more quickly than oxygen diffuses through the lawn. The border of a thick lawn has an effective oxygen concentration of 12.8%, compared to 17.1% in the center of the lawn (Fig. 5d). Thus bordering behaviours may be caused, in part, by the strong preference of *npr-1* strains for lower oxygen concentrations.

Moderate bordering behaviour is evident in N2 animals grown on thick bacterial lawns, consistent with the moderate hyperoxia avoidance that N2 exhibits on food. N2 bordering behaviour was suppressed by a shift from 21% to 7% oxygen (Fig. 4a,d) or

from 21% to other low oxygen concentrations (Fig. 5a). Conversely, bordering in the N2 background was stimulated by a shift from 7% to 21% oxygen (Fig. 4d). N2 animals aggregate for the first 20 minutes after transfer to a fresh bacterial lawn (*i.e.*, a lawn with no worms on it)(de Bono et al., 2002). This aggregation was suppressed at 7% oxygen (Fig. 4g,h). Thus oxygen acts in parallel to *npr-1*, regulating social feeding behaviours regardless of the *npr-1* genotype of the animal.

In the N2 genetic background, *gcy-35* mutants exhibited lower levels of aggregation and bordering than wild-type animals (Fig. 4c,e,g). Changes in oxygen concentration between 21% and 7% had little effect on bordering behaviour in *gcy-35* mutants (Fig. 4e). Moreover, *gcy-35* mutants aggregated less than N2 when placed on a fresh bacterial lawn under 21% oxygen (Fig. 4g). Expression of a *gcy-35* cDNA in URX, AQR, and PQR restored the oxygen sensitivity of these mutants (Fig. 4e). These results suggest that oxygen acts through *gcy-35* to regulate aggregation and bordering, a process that is antagonised by *npr-1* activity. Indeed, an independent study recently showed that *gcy-35; npr-1* double mutants do not border or aggregate(Cheung et al., 2004). Like *gcy-35* mutants, *tax-4* mutants responded poorly to changes in oxygen levels, suggesting that oxygen regulation of social feeding behaviour depends on cGMP-gated channels (Suppl. Fig. 3).

Discussion

These behavioural results demonstrate that GCY-35 is required for avoidance of hyperoxia and for oxygen-induced aggregation and bordering. Biochemical evidence suggests that GCY-35 forms a stable ferrous-oxy complex. Canonical NO-sensitive

sGCs do not bind oxygen; indeed, their inability to bind oxygen is essential to their ability to sense NO, since the NO:O_2 ratio in tissues is about 1:1000(Malinski and Taha, 1992; Malinski et al., 1993). By analogy with the NO-sensitive sGCs, we suggest that oxygen modulates GCY-35 guanylate cyclase activity, either directly or by competing with other activators like NO. Although catalytic activity remains to be demonstrated, several bacterial and archaeal haem domains mediate aerotaxis(Hou et al., 2000), and one other sGC-like haem domain, Tar4H from *Thermoanaerobacter tengcongensis,* has been found to bind oxygen(Karow et al., 2004). Our results suggest that the soluble guanylate cyclase GCY-35 may represent one member of a new class of oxygen-sensitive sGCs.

GCY-35 mediates oxygen sensing in URX, AQR, and PQR. The URX sensory neurons have dendrites that extend to the tip of the nose, suggesting that URX detects external stimuli. The AQR and PQR neurons extend dendrites with ciliated endings into the pseudocoelom, an internal, fluid-filled cavity immediately under the epithelium(White, 1986). AQR and PQR may detect internally generated stimuli or internal levels of externally produced stimuli. Based on its rate of diffusion through water, molecular oxygen should diffuse from the environment to the AQR and PQR sensory endings in less than a second.

Because oxygen diffuses rapidly through small animals like *C. elegans*, it does not become a limiting factor for respiration until it reaches external concentrations below 4%(Anderson, 1977; Van Voorhies and Ward, 2000). Above 4% oxygen, additional increases in oxygen do not affect respiration, but are likely to increase cellular oxidative damage, since the propensity to produce reactive oxygen species will increase with

oxygen concentration(Imlay, 2003). One mechanism for protecting against such damage may be a behavioural preference for lower oxygen environments. This strategy has been well-characterised in bacteria, which distribute in oxygen gradients in characteristic bands at their preferred concentration(Barak et al., 1982). In *C. elegans*, behavioural preference for lower oxygen concentrations could also result from factors unrelated to oxidative stress; for example, low oxygen may signal the presence of food in the form of actively growing bacteria that consume oxygen more quickly than it diffuses through soil.

Our results suggest that social feeding behaviour represents an integrated behavioural response to aversive hyperoxic conditions (Fig. 5e). Accumulation at the border of the lawn may represent direct aerotactic avoidance of hyperoxia. By contrast, small groups of animals are unlikely to create oxygen gradients sufficient to attract more animals. We propose that high oxygen and other aversive chemical stimuli(de Bono et al., 2002) serve as sensory triggers that can initiate social behaviour by activating chemotaxis or mechanotaxis to other animals.

An independent study found that mutations in either *gcy-35* or the related gene *gcy-36* suppress bordering and aggregation in *npr-1* mutants(Cheung et al., 2004). Together, these results suggest that oxygen regulates social behaviour by modulating the guanylate cyclase activity of GCY-35 and GCY-36. It will be interesting to see whether soluble guanylate cyclases act as neuronal oxygen sensors in other animals.

Methods

Strains, Molecular Biology, Biochemistry, and Statistics were performed using standard techniques, as described in Supplemental Methods.

Oxygen binding of bacterially-produced GCY-35(1-252). Purified bacterially-produced protein was made anaerobic in an O_2-scavenged gas train with 10 cycles of alternate evacuation and purging with purified argon and brought into an anaerobic glove bag. Ferricyanide (~100 equivalents) was added and then removed using a PD10 desalting column that had been equilibrated with 50 mM TEA pH 7.5 and 50 mM NaCl (Buffer C). The protein was then reduced using dithionite (~100 equivalents). The dithionite was then removed in the same manner. A ferrous-unligated UV/Vis absorption spectrum was recorded in an anaerobic cuvette on a Cary 3E spectrophotometer equipped with a Neslab RTE-100 temperature controller set at 10 °C. Spectra were recorded from protein in Buffer C. Fe^{+2}-O_2 protein and other gas-bound proteins were generated by exposing Fe^{+2}-unligated GCY-35(1-252) to air or other gases before recording a spectrum. Bacterial haem can assemble with recombinant eukaryotic haem-binding proteins, and since *C. elegans* cannot itself synthesise haem(Hieb et al., 1970), bacterial haem is likely the natural form for *C. elegans* guanylate cyclases.

Behavioural Assays. For gas-phase aerotaxis assays, micro devices were fabricated using the PDMS rapid prototyping technique(Duffy et al., 1998). The photolithography masks were laser-printed on silver halide films with 1/40.64 *mil* resolution, and used to produce the prototype masters in a photo-patternable epoxy (SU-8-50, Microchem Inc., Newton, MA) on silicon wafers using standard UV photolithography. The masters were silanised using vapour phase tridecafluoro-1,1,2,2-tetrahydrooctyl trichlorosilane (United

Chemical Technologies, Bristol, PA). The PDMS devices were micromolded using 2-part Sylgard 184 silicone elastomer (Dow Corning, Midland, MI) against the masters. Prior to the assay, the devices were cleaned in ethanol followed by DI water and dried overnight at 65 °C.

In each assay, 30-200 washed adult animals were placed on an NGM agar plate before the device was placed over them. Air and nitrogen gas (room temperature, 1 atm) were delivered to the source and drain chambers under laminar flow at 1 ml/min for 15-30 minutes from gas-tight syringes using a syringe pump (PHD2000, Harvard Apparatus). Although PDMS and agar are both oxygen-permeable, the diffusion rate of gases through these media is substantially smaller than the gas flux between the source and drain, and did not disrupt the oxygen gradient in gas phase. Animals at nine equally sized regions in the device were counted at the end of the assay, determined by at least two consecutive scorings (five minutes apart) yielding similar spatial distributions. Each aerotaxis data point represents 3-8 assays with 80 or more animals per assay. In assays with fewer than 80 total animals, counts from experiments done on the same day were combined for data analysis. The oxygen concentration gradient in the agar was measured using a Clark-style oxygen microelectrode with guard cathode (Chemical microsensor #1201, Diamond Microsensors), which was calibrated with standards immediately prior to each use.

For aggregation and bordering assays, 40 animals were picked onto a bacterial lawn, allowed to equilibrate for an hour, placed into a flow chamber with a constant gas flow of 150 ml/min, and exposed to 21% oxygen for at least 30 minutes. Oxygen was then adjusted to different concentrations for various periods of time at a constant flow

rate of 150 ml/min. The flow chamber was a 100 x 15 mm petri dish with a modified cover: two female luers (Biorad) were melted and glued into the ends of the cover. One luer served as the gas inlet and was connected to tubing, while the other luer was always exposed to air and served as the outlet. Gas mixes with varying concentrations of oxygen were obtained by mixing oxygen and nitrogen (99.997%) in a flowmeter (Cole-Parmer). All gases were obtained from Airgas. Images were captured every ten minutes with an Ultrachip CCTV camera (JE-7442, Javelin) mounted on a stereomicroscope (Wild M3Z, Leica). The analog camera output was connected to the RCA port on a Macintosh PowerPC 7600/132 equipped with an on-board analog/digital converter. Movies and photographs were captured with Adobe Premiere software (version 4.0.1). Bacterial lawns (OP50 strain) were grown for four days prior to the assay and were 10-13 mm in diameter. Animals within 1 mm of the edge of the bacterial lawn were scored to be in the border. Any animal that was touching at least one other animal across at least 30% of its body was scored to be in an aggregate.

For the transient aggregation experiments in Fig. 4g,h animals were placed in the flow chamber and counted immediately after transfer to a fresh bacterial lawn. Fresh bacterial lawns were 4-day-old strain OP50 lawns that had never encountered worms.

In Fig. 5c, a thin bacterial lawn (bacterial strain OP50) was produced by seeding 10 cm NGM plates that were used 8-10 hours later.

Supplemental Methods.

Strains. Strains were cultured under standard conditions(Brenner, 1974). The *gcy-35(ok769)* deletion was provided by the *C. elegans* knockout consortium and its structure confirmed by PCR across the coding region of the gene. Primer pairs with one or both primers inside the deletion amplified DNA from N2 but not *gcy-35* lysates. Primers outside the deletion amplified DNA from both strains. The deletion spans 668 base pairs from cosmid T04D3 (31961-32630), with flanking sequences ACCTTTATCTTCGTT and TTTGTTCGCCACGTT. The deletion is downstream of a large intron in *gcy-35* that contains a second gene of unknown function transcribed from the opposite strand as *gcy-35* (T04D3.5); the coding region and 1 kb upstream of this gene are intact in the deletion. The mutant strain was outcrossed six times using a linked marker and verified by PCR. Primers used for sequencing and outcrossing were CTTTCAGTCCGTTGAGCTTC and 5'CCTGGTACAGTATTTAGGCG, which yields a 935 bp product from N2 lysates and a 267 bp fragment from *gcy-35* lysates.

tax-4(ks28) and *tax-2(p691)* are point mutations that act as strong loss-of-function alleles. *tax-4(p678)* is an early stop and a presumed null allele. *npr-1(ad609)* is an EMS-induced loss-of-function allele in the N2 background; *npr-1(g320)* is the naturally occurring Val-to-Phe 215 amino acid substitution from the social feeding strain RC301, backcrossed ten times into the N2 genetic background.

Molecular Biology. *gcy-32, gcy-34, gcy-35, gcy-36,* and *gcy-37*cDNAs were generated by RT-PCR using a mixed-stage *C. elegans* cDNA library (Stratagene) as a template.

Primer design was based on predicted sequences from the annotated genome. 5' and 3' untranslated regions were determined by RACE (Roche). These cDNA sequences have been submitted to Genbank. The *gcy-35* cDNA encodes a protein of 688 amino acids.

PCR was used to amplify his-tagged GCY-35(1-252) from a full-length *gcy-35* clone. The upstream primer for GCY-35(1-252) was GGGGGGCATATGttcggctggattcacgaa and the downstream primer was ATAGTTTAGCGGCCGCatttggaaacgttttcttgataaag. The upstream primer contained a *Nde*1 restriction site and the downstream primer contained a *Not*1 site. Digested PCR products were ligated into the bacterial expression vector pET-20b (Novagen) and sequenced to confirm the absence of PCR-generated mutations.

Upstream sequences used for the promoter::GFP transgenes contained the start codons and 1.2, 1.0, 1.0 and 1.1 kb of upstream sequence for *gcy-35*, *gcy-34*, *gcy-36,* and *gcy-37*, respectively. The upstream primers all contained an *Xba*I restriction site: GCTCTAGAaacaatggggtgggcacgataga, GCTCTAGAccagagcgaatcaattgatttcaagaac, GCTCTAGAcatgatgttggtagatggggtttgg and GCTCTAGAgtgtatcagaaattcttgcaatccg for *gcy-35*, *gcy-34*, *gcy-36,* and *gcy-37*, respectively. The downstream primers contained a *Bam*HI site: CGCGGATCCatattctactctccgcaaaaaagt, CGCGGATCCattttgagaagttttttgaacagctgc, CGCGGATCCattgttgggtagcccttgtttgaattt and CGCGGATCCatatttctgtgtagtagaaaaag for *gcy-35*, *gcy-34*, *gcy-36,* and *gcy-37*, respectively. Digested PCR products were ligated into the pPD95.67 expression vector (a gift from Andrew Fire), which contains an SV40 nuclear localization signal. The promoter region was sequenced to verify accuracy. In addition, for *gcy-35*, a fragment with 3.9 kb of upstream sequence terminating in the second exon of the gene was ligated into the pPD95.77 vector. Both *gcy-35::gfp* fusion genes showed expression in similar

neurons, and the larger fusion also showed expression in pharyngeal and body wall muscles and in the excretory cell. The promoter::GFP transgenes were microinjected according to standard methods(Mello and Fire, 1995), with coinjection plasmid pRF4 (*rol-6(su1006d)*) or *elt-2::gfp* at 10ng/μl.

For rescue, the *gcy-35* cDNA was placed in pSM1, a modified pPD49.26 with extra cloning sites (S. McCarroll and C.I.B., unpublished data). The *gcy-32* or *gcy-36* promoter was inserted into this expression vector from FseI to AscI after PCR amplification from genomic DNA using the following primers: downstream primer ttggcgcgccTATATTTTCCTTTCCGCTTTC and upstream primer ttggccggccATTTCCATTCCACTGATGATGTGA for *gcy-32* and upstream primer ttggccggccATGATGTTGGTAGATGGGGTTTGG and downstream primer ttggcgcgccTGTTGGGTAGCCCTTGTTTGAATTT for *gcy-36*. The resulting plasmids were injected at 50 ng/μl (*gcy-32::gcy-35*) or 5 ng/μl (*gcy-36::gcy-35*) with 10 ng/μl *elt-2*::GFP as a co-injection marker. For rescue with a genomic fragment (Suppl. Fig 3), a PCR fragment spanning the *gcy-35* locus with 0.7 kb of upstream sequence, 1.3 kb of downstream sequence, and the entire *gcy-35* coding region was amplified from wild-type genomic DNA with the primers GAAAAAGAGCAAGGAAGAGACAGAGGG and TCTAGCGAGGAAAACGAAGAAGACGAG and injected into *gcy-35(ok769)* at 40 ng/μl with 10ng/μl *elt-2::GFP*.

Biochemistry. *E. coli* expression was performed as described previously(Zhao and Marletta, 1997) with the following modifications. Plasmids were transformed into Tuner DE3 plysS cells (Novagen). Cultures were grown until an OD_{600} of 0.5-1 and cooled to

27 °C. IPTG (Promega) was added to 10 μM and aminolevulinic acid to 1 mM. Cultures were grown overnight for 14-18 h and then harvested. Protein was purified by nickel affinity and size exclusion chromatography in the following manner. Frozen cell pellets from 3 liters of culture were thawed quickly at 37 °C and resuspended in 120 ml of Buffer A (50 mM $NaPO_4$ pH 8.0, 300 mM NaCl, 5 mM β-mercaptoethanol, 10 mM imidazole, 1 mM Pefabloc (Pentapharm) and 5% glycerol). Resuspended cells were lysed with sonication and, subsequently, with an Emulsiflex-C5 high pressure homogenizer at 20,000 psi (Avestin, Inc.). Lysed cells were centrifuged at 100,000 x g for 40 min. The supernatant was applied to Nickel NTA superflow resin (Qiagen) (10 ml) and washed with 10 column volumes of Buffer A. The his-tagged protein was eluted with modified Buffer A (containing 150 mM imidazole) at 2.5 ml/min. Fractions were selected on the basis of their color and A_{280}/A_{Soret} ratio. The eluate was concentrated to 4 ml using 15 ml 10K MWCO spin concentrators (Millipore). The concentrated proteins were applied to a pre-packed Superdex S75 HiLoad 26/60 gel filtration column (Pharmacia) that had been equilibrated with 50 mM Hepes pH 7.4, 200 mM NaCl and 5% glycerol. The flow rate was 1.4 ml/min. Fractions containing GCY-35(1-252) were pooled and stored at –70°C.

Western blotting was performed by ECL according to the manufacturer protocol (Amersham). The GCY-35 antibody was generated by immunizing rabbits with a conjugated synthetic peptide corresponding to residues 36-50 of GCY-35, and affinity purified by the manufacturer (Research Genetics).

Statistical analysis. To test statistical significance in Figures 4d-f, the first three measurements at 21% oxygen were grouped and compared to the three measurements at 7% oxygen. p-values were generated using Student's t-test. N2 bordering and *npr-1* bordering and aggregation were suppressed at 7% oxygen ($p<0.001$). *gcy-35* was significantly different from N2 ($p<0.001$), and its defect was rescued by the *gcy-32::gcy-35* transgene ($p<0.01$). All assays were completed at least three times. For panel 4g, in 21% oxygen N2 was different from *gcy-35* ($p<0.001$). For panels 4g and 4h, N2 aggregation differs in 21% and 7% oxygen ($p<0.001$).

In Figure 5d, the lawn center differs from both the agar and the lawn border by Student's t-test ($p<0.001$).

Statistical analysis of aerotaxis (Figs. 1,5) is described in Supplemental Figure 2.

Acknowledgements

We thank Jessica Feldman for valuable discussions and contributions to the aerotaxis assay, Martin Hudson and David Morton for advice and discussions, Catherine Ross, Scott Nicholls, and Mike Miazgowicz for technical assistance, Manuel Zimmer for the *gcy-32* promoter, Steven McCarroll for the pSM1 vector, the *C. elegans* Knockout Consortium and *Caenorhabditis* Genetics Center (CGC) for the *gcy-35(ok769)* mutant strain, and Benny Cheung and Mario de Bono for sharing their results prior to publication. JMG was supported by a Howard Hughes Medical Institute Predoctoral Fellowship. AJC was supported by an NSF Predoctoral Fellowship. CIB is an Investigator of the Howard Hughes Medical Institute. This work was supported by funding from the Howard Hughes Medical Institute (to CIB) and by the LDRD fund from

the Lawrence Berkeley National Lab (to MAM). The authors declare that they have no competing financial interests in this work.

Correspondence may be addressed to C.I.B. (cori@itsa.ucsf.edu) or M.A.M. (marletta@berkeley.edu).

Figure legends

Fig. 1: gcy-35 mutants are defective in hyperoxia avoidance.

a. Gas-phase PDMS aerotaxis device, top view. A gas-phase gradient was established by diffusion along the long axis of the device.

b. Measured oxygen concentrations in aerotaxis device, and side view of device.

c. Wild-type N2 animals accumulate at intermediate oxygen concentrations.

d. Defective hyperoxia avoidance in *gcy-35* mutants, and rescue by *gcy-32::gcy*-35 expression in URX, AQR, and PQR.

e. Defective hyperoxia avoidance in *tax-4* and *tax-2* mutants.

f. Similar oxygen preference of N2, *npr-1(g320),* and *npr-1(ad609).*

Error bars denote standard error of the mean (SEM). Statistical analysis, Fig. S2.

Fig. 2: *gcy-35::gfp* is expressed in URX, AQR, PQR, and other sensory neurons.

a. Lateral view of the anterior body showing URX, AQR, SDQR, and BDU neurons. Anterior is at left and ventral is down.

b. Ventral view of the tail showing PQR and ALNL/R neurons. The more posterior cells may be PLM neurons, the sisters of ALNL/R, or PLN neurons.

Fig. 3: Characterisation of GCY-35(1-252) binding to gases.

a. UV/vis spectroscopy of GCY-35(1-252). Black broken trace shows anaerobic spectrum of ferrous-unligated complex (peaks at 430 and 559 nm). Solid red trace shows the same sample after exposure to air, and is indicative of a ferrous-oxy complex (peaks at 415, 542, and 578 nm).

b. Purification of GCY-35(1-252):His. Left, Coomassie-stained gel. Right, Western blot with affinity-purified anti-GCY-35 antisera, lanes at 10-fold different dilutions.

c. Comparison of spectroscopic data for GCY-35(1-252), soluble GC(Stone and Marletta, 1994), hemoglobin(Di Iorio, 1981), and *Thermoanaerobacter tengcongensis* Tar4H(Karow et al., 2004) unliganded and in the presence of CO, NO, and O_2.

Fig. 4: Oxygen stimulates GCY-35-dependent aggregation and bordering.

a-c. Animals equilibrated at 21% oxygen or 7% oxygen for 30 minutes. a. N2 b. *npr-1(ad609)* c. *gcy-35(ok769)*.

d-f . Oxygen shifts from 21%—7% —21% (dotted lines).

d,f. 7% oxygen suppresses bordering in N2 and *npr-1* strains and aggregation in *npr-1* strains.

e. Reduced oxygen sensitivity of bordering in *gcy-35(ok769)*, and rescue by *gcy-32::gcy-35* transgene.

g,h. Aggregation of N2 and *gcy-35(ok769)* immediately after transfer to a fresh bacterial lawn in 21% or 7% oxygen.

Error bars denote SEM. Statistical analysis in Supplemental Material.

Fig. 5: Regulation of oxygen responses by food.

a,b. Bordering and aggregation during oxygen shifts (dotted line).

c. Aerotaxis on a thin bacterial lawn. N2 aerotaxis is suppressed.

d. Oxygen concentrations in and near a thick OP50 bacterial lawn.

Error bars denote standard error of the mean (SEM).

e. Model for oxygen regulation of behaviour. Oxygen directly or indirectly regulates GCY-35; cGMP activates the TAX-2/TAX-4 cGMP-gated channel in URX, AQR and PQR to promote hyperoxia avoidance, bordering, and aggregation. The neuropeptides FLP-18/21 (possibly released by pharyngeal neurons during feeding(Rogers et al., 2003)) activate the neuropeptide receptor NPR-1, which inhibits URX, AQR, and PQR.

Supplemental Figure legends

Supplemental Fig. 1: gcy-32, gcy-34, gcy-35, gcy-36, and gcy-37 are C. elegans homologs of rat sGCs. a. Residues from the predicted N-terminal heme binding domain. GCY-32, GCY-34, GCY-35, GCY-36, and GCY-37 have a key residue, rat β1 H105 (boxed), which ligates the heme cofactor, suggesting that these predicted cyclases bind heme. b. Residues from the predicted C-terminal catalytic domain. Canonical mammalian sGC is a heterodimer composed of α1 and β1 subunits(Denninger and Marletta, 1999); catalytically-active, NO-sensitive β2 homodimers and an 2 1 heterodimer have also been reported(Gibb et al., 2003; Koglin et al., 2001; Russwurm et al., 1998). A structural homology model comparing the catalytic domain of sGC (α1β1) with the crystallized adenylate cyclase catalytic domain(Sunahara et al., 1998; Tesmer et

al., 1997) predicts that all four residues involved in catalysis (D485 and D529 from rat α1, C541 and E473 from rat β1) are conserved in *C. elegans* GCYs, suggesting that the *C. elegans* GCYs could be catalytically active. Mutagenesis results from both α1 and β1 are incorporated; black numbers denote the sGC for which function was confirmed by mutagenesis (e.g. α1 485 corresponds to β1 426; mutagenesis was conducted only on α1, so numbering on β1 is in grey). A horizontal box in *gcy-35* denotes the deletion in *gcy-35(ok769)*. The alignment was generated using DNASTAR's MegAlign program and the Clustal W method. Accession numbers are: rat 1.U60835, rat 1.P20595, rat 2.P22717.

Supplemental Fig. 2: Statistical analysis of aerotaxis data from Fig. 1, Suppl. Fig. 3, and other experiments. Aerotaxis assays were scored in nine bins of equal size that spanned the linear gradient from 0-21% oxygen. To generate a hyperoxia avoidance index, we compared the distribution of animals between medium oxygen (bins 5-7, 4.66-11.67%) and high oxygen (bins 1-4, 11.67-21%), correcting for the smaller total area covered by bins 5-7 by calculating the average fraction of animals in each bin. A hyperoxia avoidance index was calculated as (Medium-High)/(Medium+High); hyperoxia avoidance of 1.0 represents complete exclusion of animals from bins 1-4 in the aerotaxis assay, 0.0 represents indifference to hyperoxia and –1.0 represents complete exclusion from bins 5-7. Wild-type animals exhibited no preference in the absence of an oxygen gradient (N2 air control). Results were analyzed by ANOVA and Bonferroni t-test. * indicates strains or conditions that were significantly defective in avoidance of hyperoxia compared to N2 in the absence of food ($p<0.05$). + indicates transgenic *gcy-35* strains that were significantly rescued compared to *gcy-35(ok769)* ($p<0.05$). The *gcy-35*

defect was fully rescued by the *gcy-35* cDNA expressed in URX, AQR, and PQR under the *gcy-32* promoter (2 lines), and was partially rescued by a *gcy-36::gcy-35* clone (1 line) and a *gcy-35* genomic clone (1 line). The *tax-4(ks28)* defect was fully rescued by *tax-4* expressed in URX, AQR and PQR under the *gcy-32* promoter(Coates and de Bono, 2002). N2 animals on food were highly defective in hyperoxia avoidance (*), whereas *npr-1(g320)* and *npr-1(ad609)* on food had normal or enhanced hyperoxia avoidance (**).

Supplemental Fig. 3: A genomic fragment rescues the *gcy-35* defect, and *tax-2* and *tax-4* have defects. a. Aerotaxis responses of additional rescued *gcy-35 (ok769)* transgenic lines: *gcy-32::gcy-35* line B, *gcy-36::gcy-35*, and a *gcy-35* genomic clone. b. Aerotaxis responses of *gcy-35(ok769) tax-4(ks28)* double mutants, *tax-4(p678)* mutants, *tax-2(p691) tax-4(p678)* double mutants, and *tax-2(ks28)* animals rescued by a *gcy-32::tax-4* transgene(Coates and de Bono, 2002) (*gcy-32* is expressed in URX, AQR, and PQR). *tax-4(p678)* is an early stop codon resulting in truncation of the channel. *tax-4(ks28)* is a point mutation in *tax-4* that may interfere with *tax-2* function as well as *tax-4*. *tax-2(p691)* is a point mutation in the pore domain that acts as a strong loss-of-function allele. c,d. Bordering (c) and aggregation (e) were not observed at 21% or 7% oxygen in *tax-4(ks28)* mutants or *tax-2(p691); tax-4(p678)* double mutants. Experiments were performed as described in Figures 1 and 4.

Figure 3.1

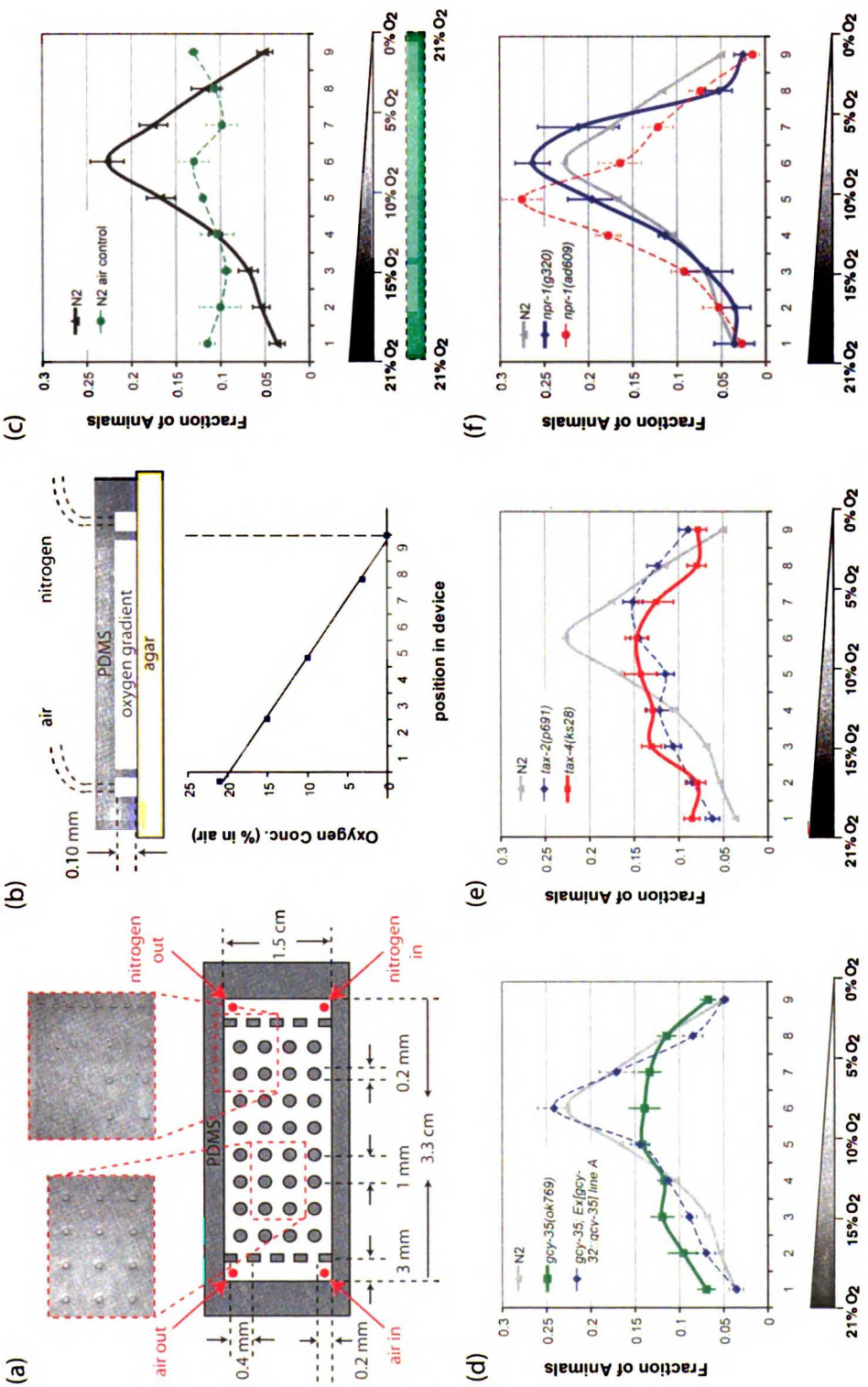
(a)
nitrogen out
nitrogen in
air out
air in
PDMS
1.5 cm
0.4 mm
0.2 mm
0.2 mm
3 mm
1 mm
0.2 mm
3.3 cm
(b)
air
nitrogen
0.10 mm
PDMS
oxygen gradient
agar
Oxygen Conc. (% in air)
position in device
(c)
N2
N2 air control
Fraction of Animals
21% O2
15% O2
10% O2
5% O2
0% O2
(d)
N2
gcy-35(ok769)
gcy-35; Ex[gcy-32::gcy-35] line A
Fraction of Animals
(e)
N2
tax-2(p691)
tax-4(ks28)
Fraction of Animals
(f)
N2
npr-1(g320)
npr-1(ad609)
Fraction of Animals

Figure 3.2

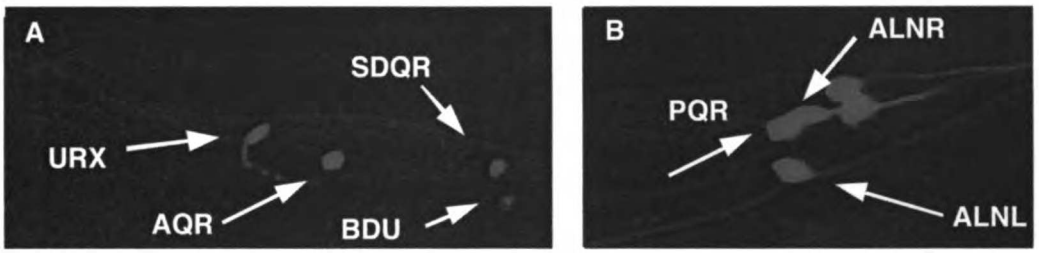

Figure 3.3

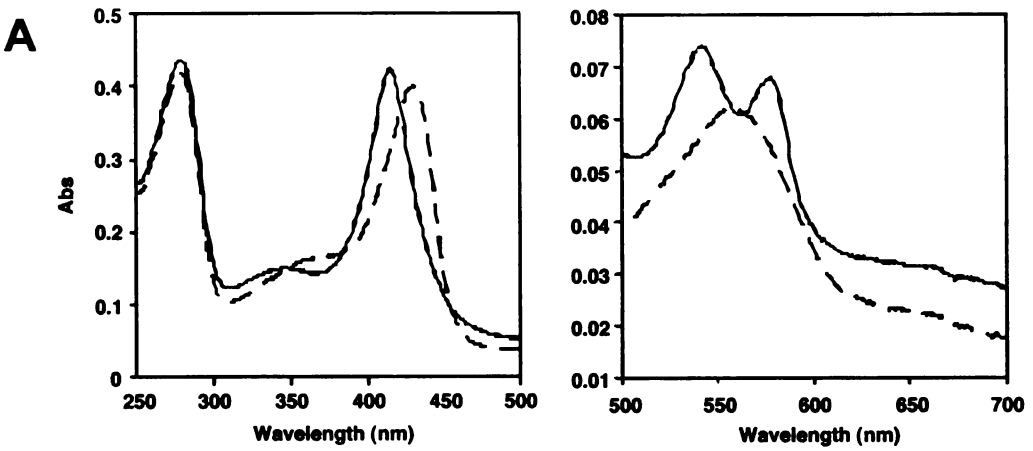

B

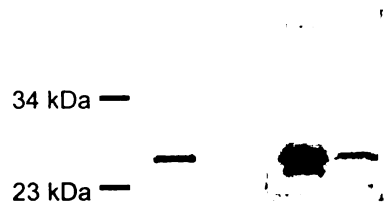

C

Ligand	Protein	Soret	α	β
None	sGC (α1β1)	431	555	
	*Tf*Tar4H	431	565	
	Hb	430	555	
	GCY-35(1-252)	430	559	
O_2	sGC (α1β1)	Does not bind		
	*Tf*Tar4H	416	556	591
	Hb	415	541	576
	GCY-35(1-252)	415	542	578
NO	sGC (α1β1)	398	537	572
	*Tf*Tar4H	420	547	575
	Hb	418	545	575
	GCY-35(1-252)	415/400	533	568
CO	sGC (α1β1)	423	541	567
	*Tf*Tar4H	424	544	565
	Hb	419	540	569
	GCY-35(1-252)	421	538	564

Figure 3.4

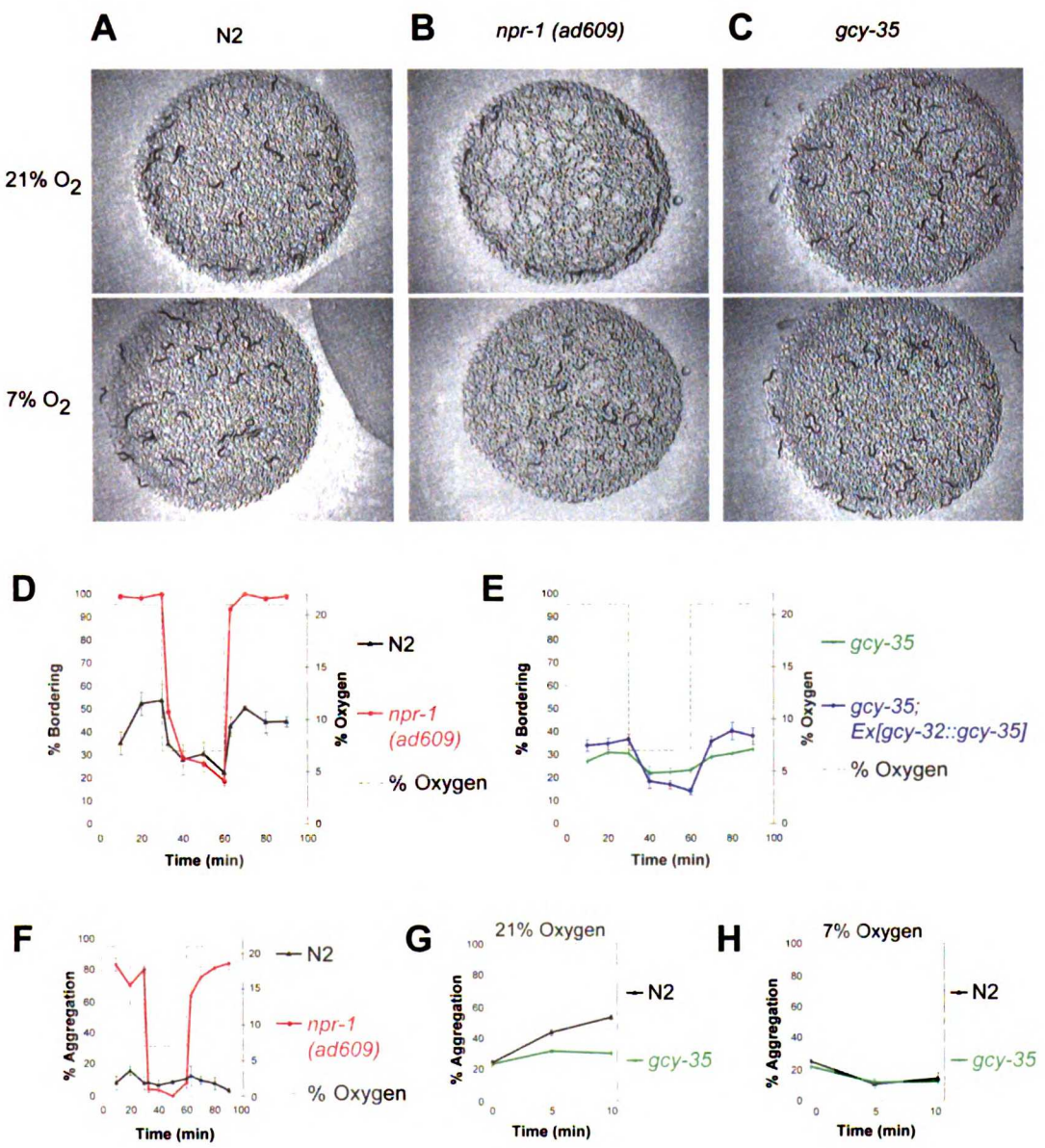
A
N2
B
npr-1 (ad609)
C
gcy-35
21% O2
7% O2
D
% Bordering
% Oxygen
Time (min)
N2
npr-1 (ad609)
% Oxygen
E
% Bordering
% Oxygen
Time (min)
gcy-35
gcy-35; Ex[gcy-32::gcy-35]
% Oxygen
F
% Aggregation
Time (min)
N2
npr-1 (ad609)
% Oxygen
G
21% Oxygen
% Aggregation
Time (min)
N2
gcy-35
H
7% Oxygen
% Aggregation
Time (min)
N2
gcy-35

Figure 3.5

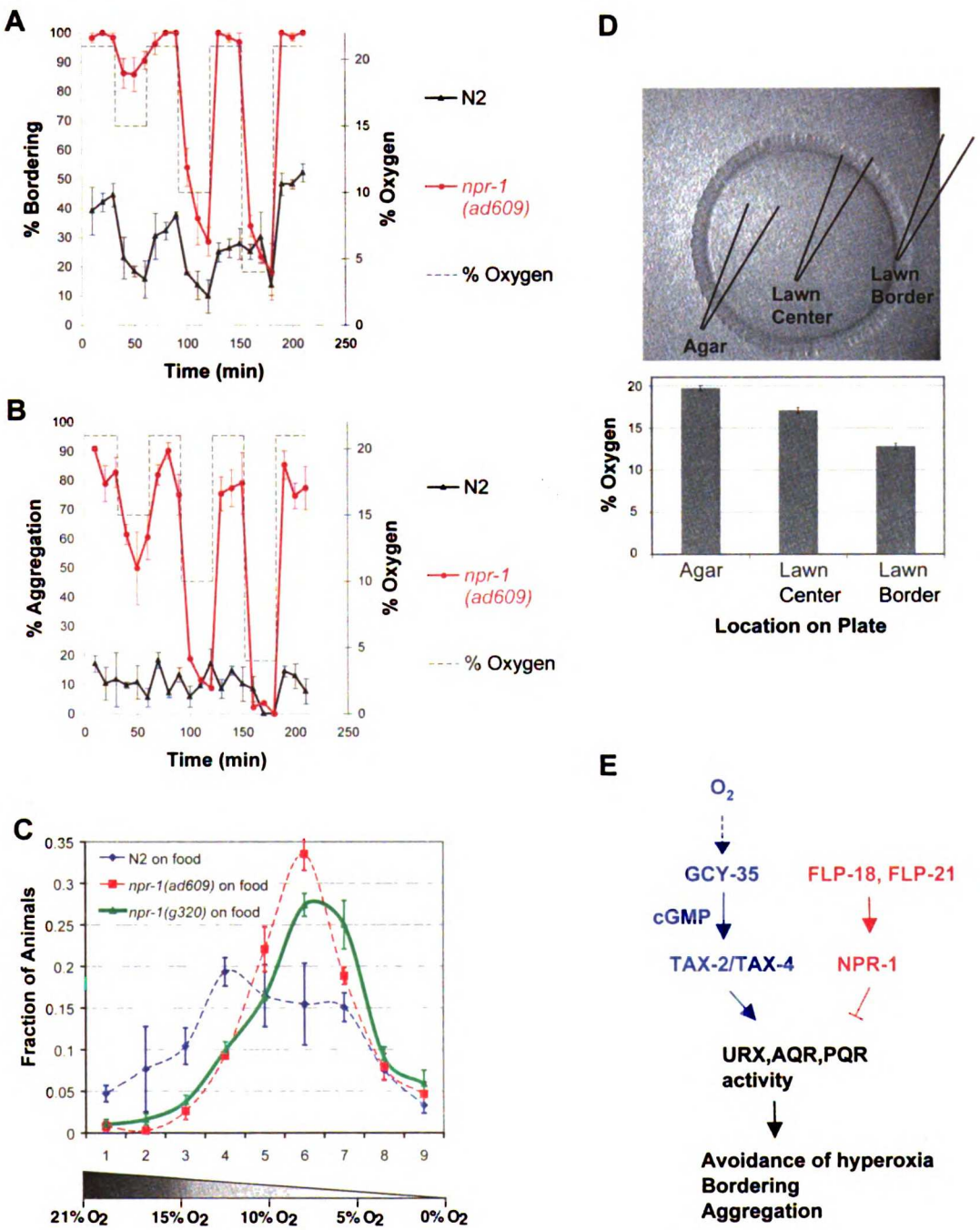
A
% Bordering
% Oxygen
Time (min)
N2
npr-1 (ad609)
% Oxygen
B
% Aggregation
% Oxygen
Time (min)
N2
npr-1 (ad609)
% Oxygen
C
Fraction of Animals
N2 on food
npr-1(ad609) on food
npr-1(g320) on food
21% O2
15% O2
10% O2
5% O2
0% O2
D
Agar
Lawn Center
Lawn Border
% Oxygen
Agar
Lawn Center
Lawn Border
Location on Plate
E
O2
GCY-35
FLP-18, FLP-21
cGMP
TAX-2/TAX-4
NPR-1
URX,AQR,PQR activity
Avoidance of hyperoxia
Bordering
Aggregation

Supplemental Figure 3.1

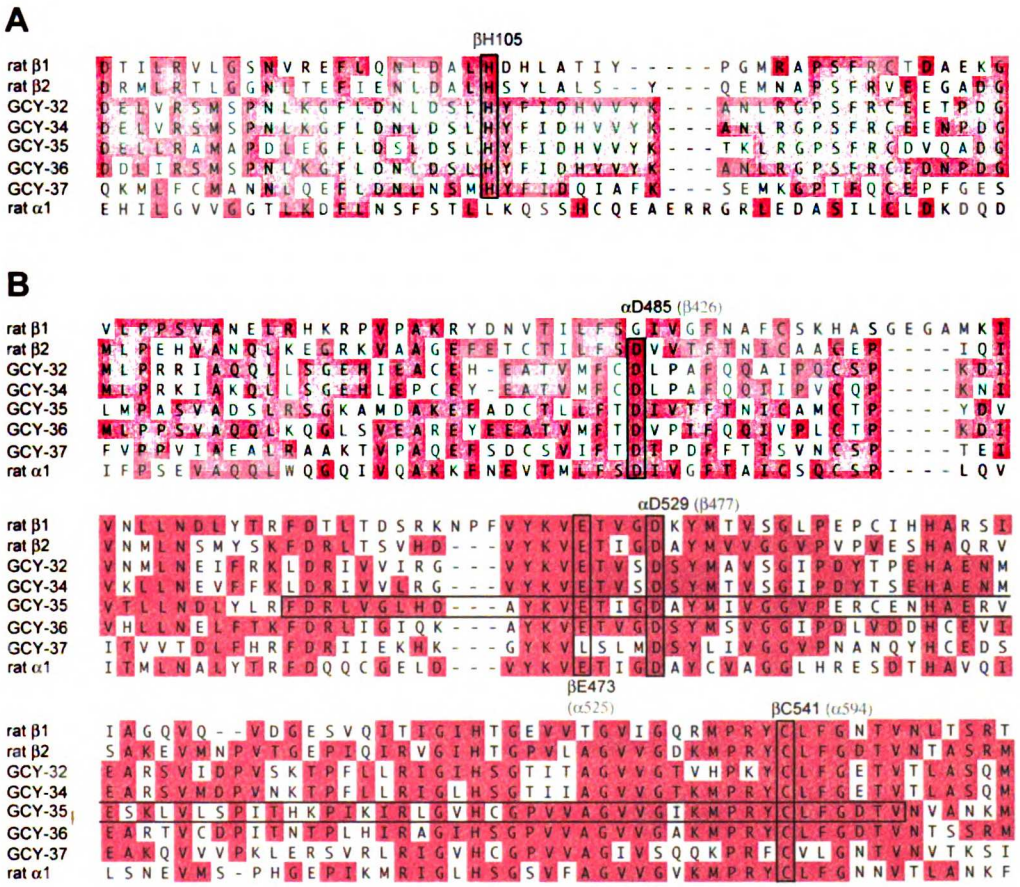

Supplemental Figure 3.2

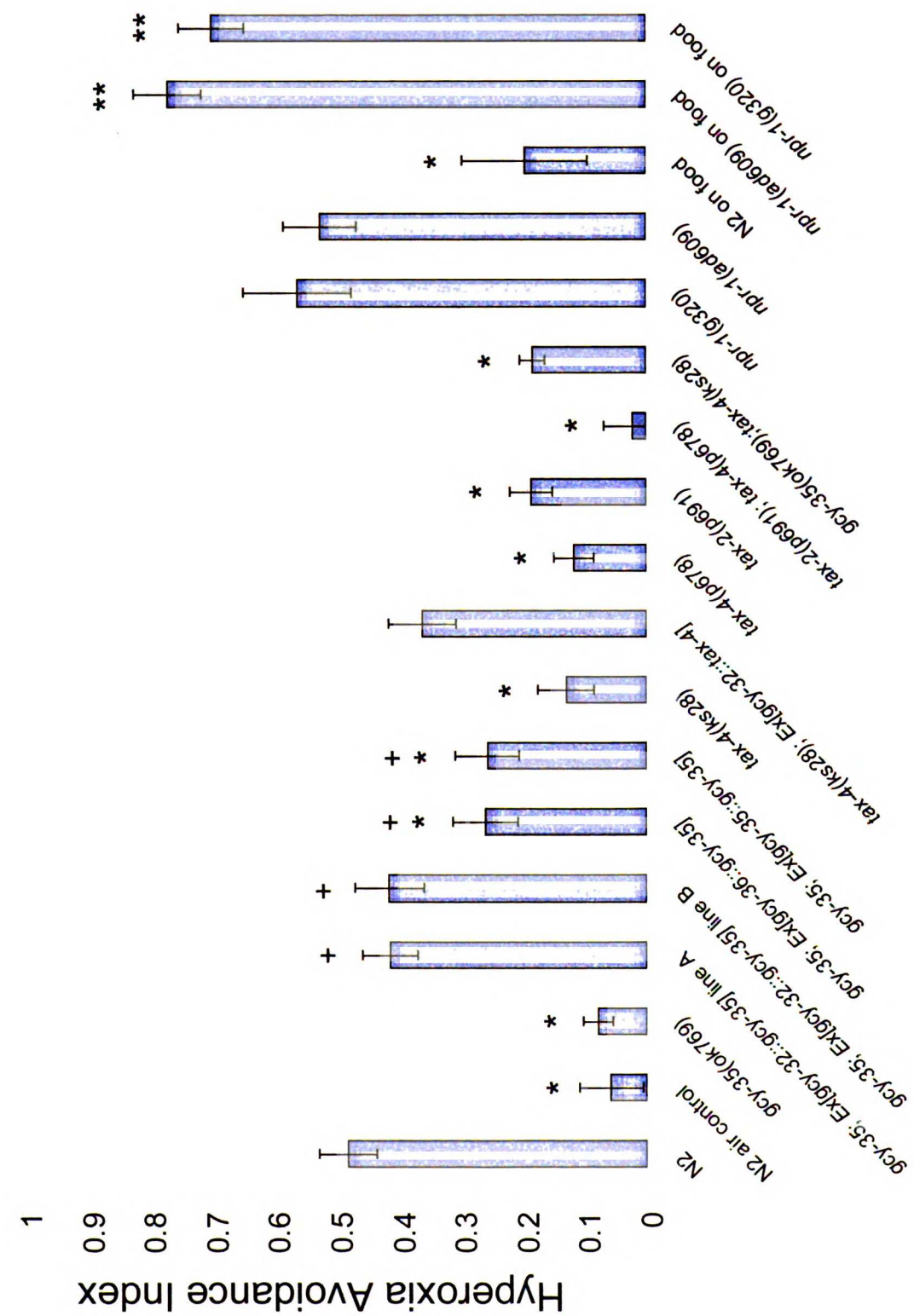

Supplemental Figure 3.3

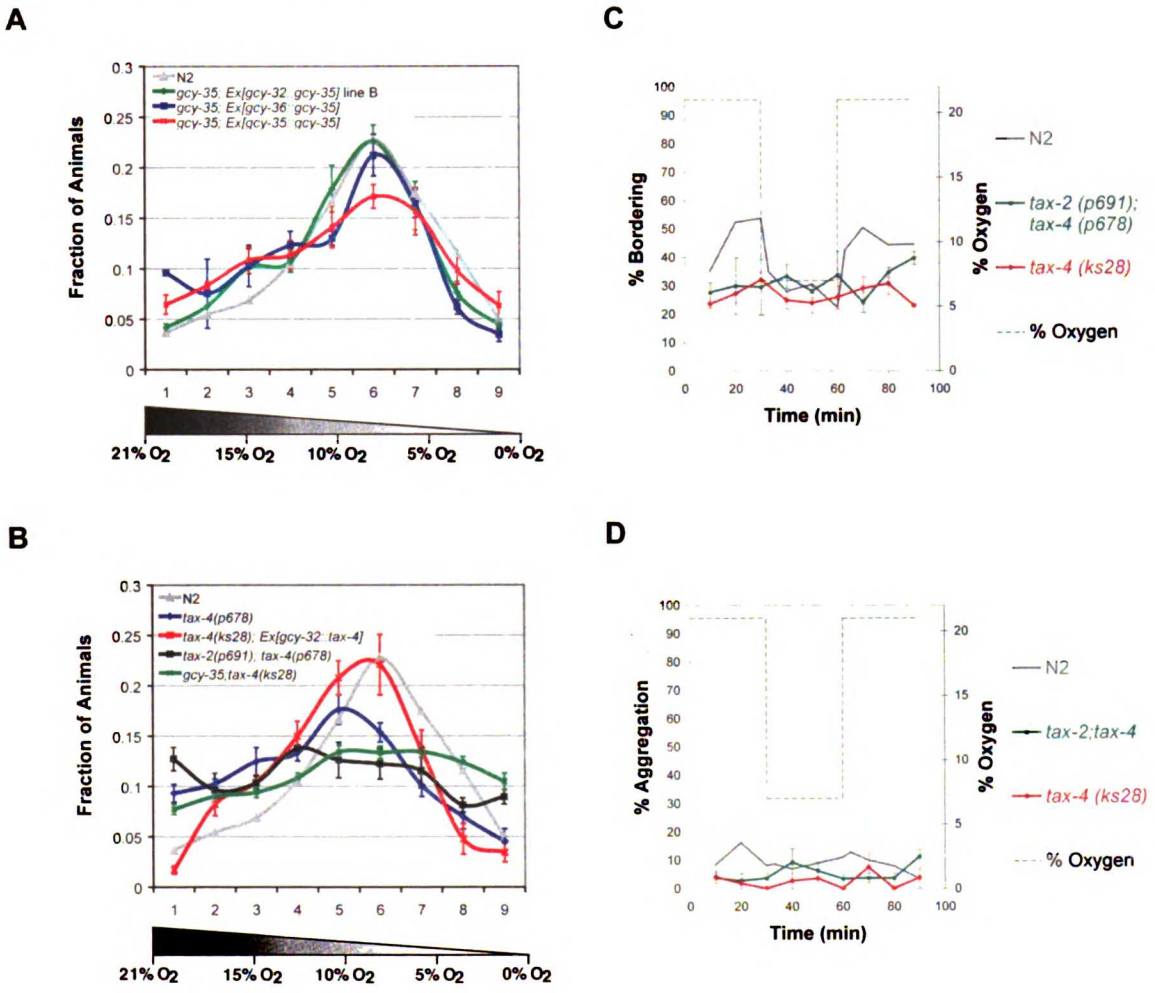

Chapter 4 – Conclusions and Future Directions

Disentangling C. elegans *Circuits – Beyond Ablations and Behavior*

From a circuit perspective, one of the more interesting future directions concerns interneuron and motor neuron function. How do *C. elegans* neurons integrate different inputs, and how is memory of recent stimuli encoded in the system? How are distinct behaviors like reversals and omega turns coupled? How is speed controlled at the level of the motor neuron pattern generator?

These questions are difficult to address using solely ablations and behavior for two reasons. First, there are many motor neurons within some of the motor neuron classes, and ablating all neurons within a class is a challenge. Second, it is difficult to separate the role of an interneuron or motor neuron in executing a task from any potential role in regulation of the task. Are AVA-ablated animals slow or just uncoordinated? To what extent does AVA regulate reversal frequency in addition to being required for reversals themselves? AVA in particular is one of the most important neurons in *C. elegans*, since it is required for reversals, which are integral to a large number of behaviors. In addition, it appears to be one of the few conduits for information from the head to reach the ventral nerve cord. AVA expresses several glutamate receptors, including two AMPA/kainate glutamate receptors, as well as two NMDA-type receptors. Mutants are already available in several of these genes. These mutants, coupled with cell-specific rescue, could do much to answer questions that ablations alone are too crude to address.

There are many examples of using genetic and molecular strategies to follow up on

ablation results, including the *C. elegans* touch circuit and *C. elegans* chemosensation, as well as very recently an example based on the work in Chapter 2 of this thesis. Identification of neurons involved in navigation behaviors makes it possible to understand the same circuit in more molecular detail. Sreekanth Chalasani in the lab has tested a list of mutants in neurotransmitter receptors and neurotransmitter synthetic machinery for defects in exploratory behaviors. By comparing the mutant defects with ablation data for different cells in the circuit as well as expression data for the genes in question, he has identified likely neurotransmitters and receptors for a subset of neurons in the circuit. He has confirmed these results with cell-specific rescue. To date, studies of reversal frequency have been focused mostly on longer-term responses involved in exploratory behavior. One of the most interesting directions made possible with the developing molecular understanding is to begin to address how reversals and turns are controlled acutely during chemotaxis.

Sreekanth's work is an example of how neurotransmitter receptor mutants promise to be a useful tool in understanding circuits in *C. elegans*. With the knockout consortia, the community is reaching a point where it may in the foreseeable future have mutants in every neurotransmitter receptor. Of the existing mutants, many have yet to be outcrossed or characterized at all. But such a panel of mutants would be a valuable resource for studying any circuit. Receptors are often quite specifically expressed, and when they are not, they can be cell-specifically rescued. In sum, they should account for all synaptic signaling. The innexins are putative components of *C. elegans* gap junctions; a panel of innexin knockouts could serve a similar function for dissecting electrical signaling

components in circuits.

Imaging neuronal activity also promises to offer more subtle understanding of the role of different neurons in circuits. Imaging is complementary to behavior, since behavior reveals the final output of a circuit, while imaging has the potential to reveal the activity of each of the components. Using calcium indicators, Sreekanth Chalasani and Nikos Chronis are imaging the chemotaxis/navigation circuits in response to food and odor, and it will be fascinating to see what these experiments reveal about circuit function. Our approach in Chapter 2 did not succeed in identifying the roles of many neurons, including the interneurons RIA and SAA and the motor neurons RMD, even though these neurons have many connections with neurons important for navigation. It will be interesting and hopefully informative to see if these cells are activated by upstream neurons in the navigational circuit despite not being important for the behavior. It should also be informative to use imaging to see what kinds of stimuli activate these and other neurons with poorly understood function. Hopefully, imaging will represent a complement to ablations in identifying the roles of neurons with unknown functions.

One of the most interesting future directions involves the differences between reversal and omega bend behaviors on and off food. Although the majority of the work in Chapter 2 is focused on a time course after removal from food, one difference between on and off food behavior is clear. Many manipulations of the circuit alter the off food behavior, but only a few alter on food behavior, despite the fact that these manipulations in sum account for a reasonable fraction of the known neurons for sensing food-related

stimuli. In addition, chemotaxis, which is likely to be mediated by the same or by a similar circuit, is suppressed by food (Cori Bargmann, personal communication). Thus, it is possible that the entire navigational circuit is shut down in the presence of food. Alternatively, the reversals and omega turns may no longer be the right behavioral metric to measure circuit output. Worm behavior on food can be divided into roaming and dwelling states (Fujiwara et al., 2002), and some manipulations performed in Chapter 2 do affect these states; namely, AIY ablations and *osm-6* mutations increase the percent of time spent dwelling (data not shown). Thus, roaming and dwelling (or some other as yet unidentified behavior) may be controlled by the navigational circuit when food is present. It would be interesting to see what neurons and pathways are necessary to change this circuit in the presence of food. Candidate pathways are those that suppress aerotaxis on food, although the wiring diagram indicates that aerotaxis is likely to be a completely different upstream circuit. Other candidate pathways include the dopamine and serotonin pathways known to slow worms down when they encounter food (Sawin et al., 2000).

Understanding C. elegans *Oxygen Behaviors*

Our finding that *C. elegans* aerotaxis in gradients is altered by food in an *npr-1*-dependent manner (Figure 3.5c) raises questions about how food regulates aerotaxis. Andy Chang in the Bargmann lab is taking a candidate genetic approach to understanding aerotaxis and has already identified other genes involved in food-regulation of aerotaxis. He has also identified a distributed circuit that controls aerotaxis, with additional sensory neurons and signal transduction molecules that contribute along with URX, AQR, and

PQR and the GCYs.

Although our results focused on avoidance of hyperoxia, the finding that aerotaxis involves avoidance of both high and low oxygen (Figure 3.5c), is an entry into questions about how hypoxia is sensed and avoided. This project is being pursued by Greg Lee in the Bargmann lab. *C. elegans* is a good system for identifying molecules, and a large outstanding question in the oxygen-sensing field asks how many additional proteins are oxygen sensors. One of the most promising future directions from our work is to do behavioral screens to identify other sensors. Hypoxia is particularly promising for screening, since in candidate approaches our lab have yet to identify any specific sensor important for hypoxia avoidance.

The finding that a soluble guanylate cyclase (sGC) seemed to be sensing oxygen raises many biochemical questions, such as whether cyclase activity is directly regulated by oxygen, whether oxygen inhibits or stimulates activity, and how different cyclases may differ in their responses to oxygen. These questions are being pursued by Shirley Huang in Michael Marletta's lab.

To some extent, the biochemical role of sGCs can be addressed *in vivo* with imaging technologies. More importantly, imaging can also reveal how oxygen influences neuronal activity and release of neurotransmitters, as well as how downstream interneurons respond to oxygen stimuli. These experiments are being performed by Manuel Zimmer in the Bargmann lab, who is using calcium indicators as a proxy for the

activity of sensory neurons and interneurons involved in oxygen behaviors. cGMP imaging will be attempted by Navin Pokala in the Bargmann lab working with Manuel.

The role of soluble guanylate cyclases in oxygen-sensing raises questions about what other animals use these molecules for sensing oxygen. These questions have been addressed in part by David Morton, who has found a role of sGCs in *Drosophila* in oxygen behaviors (personal communication) and who has data hinting at oxygen-regulated activity (Morton, 2004a). One clue comes from a residue with a role in oxygen-binding in an sGC-related bacterial protein from Thermoanaerobacter tengcongensis (Pellicena et al., 2004). The same residue is necessary and sufficient to convert an NO-sensitive cyclase into one that also detects oxygen (Boon et al., 2005). This residue, Tyr-140 in the *T. tengcongensis* protein, is lacking in soluble guanylate cyclases in most mammals with sequenced genomes, including humans, rats, and mice. However, Tyr-140 is present in sGCs from many animals, including insects and fish, both of which live in oxygen-variable environments. It will be interesting to see whether other animals use sGCs as oxygen sensors and whether they are typically involved in behavioral responses to oxygen or can also be involved in physiological responses.

Preliminary experiments conducted in collaboration with Sreekanth Chalasani and Jim Hudspeth found that mRNAs encoding an alpha2 and beta2 sGC in Zebrafish had identical expression patterns and were expressed notably in sensory clusters in the lateral line sensory organ, which is a sensory organ that can detect water currents and mediate avoidance of predators and other behaviors. This finding raises the interesting possibility

that fish sense oxygen via the lateral line and thereby possess an internal representation of external oxygen concentrations as detailed as their representation of water currents.

Identifying Additional Behaviors in C. elegans

Much of *C. elegans* behavior is devoted to understanding the function of particular genes by assessing their role in particular behaviors. This type of work is obviously important. Less attention has been devoted to understanding what behaviors are important to *C. elegans* and developing new assays to measure these behaviors.

Fully understanding the behavior of an animal requires understanding the full range of behaviors that are important for the survival of the animal. We are likely to be ignorant about a great deal of *C. elegans* behavior. Two lines of evidence support this idea. First, there are dozens of neurons whose functions are not known, and there are thousands of genes expressed in the nervous system whose roles are not known. Although these cells and genes may be important for previously identified behaviors, the circuitry would suggest that many of the sensory neurons at least are reserved for other functions, since they are often not directly connected to neurons involved in known behaviors.

The second reason we are likely to be ignorant of much of *C. elegans* behavior is that our experiments represent only a small fraction of the range of experience a worm is likely to encounter in the soil. The study of *C. elegans* behavior is limited by unknown differences between the laboratory, where experiments are conducted, and the natural environment,

where worms have evolved. Still, more could be done to bridge this gap. All but a small handful of behavioral experiments have been performed with worms grown on two strains of *E. coli*, which is not likely to be a primary food source in nature. Some of the most interesting experiments are the exception to this rule (Zhang et al., 2005)(Shtonda and Avery, in press).

Most behaviors are radically altered by the presence of food, including egg-laying, locomotion, pharyngeal pumping, and defecation. But the character of food in nature is likely to differ in many regards from that in the laboratory, even when the strain itself is the same. As one example, we find in Chapters 3 and 4 that oxygen can have a large impact on behavior. In the lab, food and worms are placed at an agar-air interface, which is likely to have much more oxygen than similar amounts of food buried in the soil.

Another reason the identification of new behaviors is important is that understanding *C. elegans* behavior will ideally involve understanding how each neuron in the worm contributes to behavior. But how can the function of each neuron be known? To date, neuronal functions have been discovered by studying behaviors such as avoidance of touch (Chalfie et al., 1985), chemotaxis to odors or salts (Bargmann et al., 1993; Bargmann and Horvitz, 1991a), or exploratory behavior, as in this work and related studies. Once a behavior has been identified, it is possible to identify the cells that are required to execute it. Thus, the dozens of neurons with no known or hypothesized function may be identified in a similar manner.

How does this work in detail? Sensory neurons involved in a novel behavior can be identified with ablations, if gene expression or anatomy provide good clues. In more difficult cases, sensory neurons can be identified through rescue of mutants such as the cilia-requiring *osm-6*, which is causes defects in most sensory neurons(Fujiwara et al., 2002). In this type of approach, rescue can be tried first with relatively broadly expressed promoters and later narrowed down with more specific ones or coupled with ablations.

Once sensory neurons have been found, downstream circuits can be identified by examining the wiring diagram and ablating interneurons immediately downstream or further downstream, as was done in this work (Chapter 2). Finally, by dissecting the motor patterns required for complex behaviors, the motor circuits themselves can be understood, as was attempted in a limited fashion here (Figure 2.5).

A final obvious but important reason to identify new behaviors is that screening with new behaviors will help identify new genes.

The study of behavior in *C. elegans* has the potential to connect understanding from biochemical, molecular, anatomical, genetic, imaging, and hopefully physiological studies to create a unified view of the behavior of an organism. Such a unified view is a long way off and should include detailed understanding of cellular signaling, adaptation in cells and circuits, network function, and motor patterns including pattern generation. Hopefully, an integrated view will be achieved and will inform studies in far more complex systems.

References

Agron, P. G., Ditta, G. S., and Helinski, D. R. (1993). Oxygen regulation of nifA transcription in vitro. Proc Natl Acad Sci U S A *90*, 3506-3510.

Anderson, G. L. a. D., D. B. (1977). Critical Oxygen Tension of *Caenorhabditis elegans*. *Journal of Nematology 9*, 253-256.

Barak, R., Nur, I., Okon, Y., and Henis, Y. (1982). Aerotactic response of Azospirillum brasilense. J Bacteriol *152*, 643-649.

Bargmann, C. I., and Avery, L. (1995). Laser killing of cells in Caenorhabditis elegans. Methods Cell Biol *48*, 225-250.

Bargmann, C. I., Hartwieg, E., and Horvitz, H. R. (1993). Odorant-selective genes and neurons mediate olfaction in C. elegans. Cell *74*, 515-527.

Bargmann, C. I., and Horvitz, H. R. (1991a). Chemosensory neurons with overlapping functions direct chemotaxis to multiple chemicals in C. elegans. Neuron *7*, 729-742.

Bargmann, C. I., and Horvitz, H. R. (1991b). Control of larval development by chemosensory neurons in Caenorhabditis elegans. Science *251*, 1243-1246.

Barr, M. M., DeModena, J., Braun, D., Nguyen, C. Q., Hall, D. H., and Sternberg, P. W. (2001). The Caenorhabditis elegans autosomal dominant polycystic kidney disease gene homologs lov-1 and pkd-2 act in the same pathway. Curr Biol *11*, 1341-1346.

Bastiani, C. A., Gharib, S., Simon, M. I., and Sternberg, P. W. (2003). Caenorhabditis elegans Galphaq regulates egg-laying behavior via a PLCbeta-independent and serotonin-dependent signaling pathway and likely functions both in the nervous system and in muscle. Genetics *165*, 1805-1822.

Berg, H. C., and Brown, D. A. (1972). Chemotaxis in Escherichia coli analysed by three-dimensional tracking. Nature *239*, 500-504.

Bickler, P. E., and Donohoe, P. H. (2002). Adaptive responses of vertebrate neurons to hypoxia. J Exp Biol *205*, 3579-3586.

Boon, E. M., Huang, S. H., and Marletta, M. A. (2005). A molecular basis for NO selectivity in soluble guanylate cyclases. Nature Chemical Biology *1*, 53-59.

Brenner, S. (1974). The genetics of Caenorhabditis elegans. Genetics *77*, 71-94.

Brockie, P. J., Mellem, J. E., Hills, T., Madsen, D. M., and Maricq, A. V. (2001). The C. elegans glutamate receptor subunit NMR-1 is required for slow NMDA-activated currents that regulate reversal frequency during locomotion. Neuron *31*, 617-630.

Chalfie, M., Sulston, J. E., White, J. G., Southgate, E., Thomson, J. N., and Brenner, S. (1985). The neural circuit for touch sensitivity in Caenorhabditis elegans. J Neurosci *5*, 956-964.

Cheung, B. H., Arellano-Carbajal, F., Rybicki, I., and de Bono, M. (2004). Soluble guanylate cyclases act in neurons exposed to the body fluid to promote C. elegans aggregation behavior. Curr Biol *14*, 1105-1111.

Coates, J. C., and de Bono, M. (2002). Antagonistic pathways in neurons exposed to body fluid regulate social feeding in Caenorhabditis elegans. Nature *419*, 925-929.

Coburn, C. M., and Bargmann, C. I. (1996). A putative cyclic nucleotide-gated channel is required for sensory development and function in C. elegans. Neuron *17*, 695-706.

Croll, N. A. (1975). Components and patterns in the behaviour of the nematode *Caenorhabditis elegans*. J Zoo Lond *176*, 159-176.

Culotti, J. G., and Russell, R. L. (1978). Osmotic avoidance defective mutants of the nematode Caenorhabditis elegans. Genetics *90*, 243-256.
de Bono, M., and Bargmann, C. I. (1998). Natural variation in a neuropeptide Y receptor homolog modifies social behavior and food response in C. elegans. Cell *94*, 679-689.
de Bono, M., Tobin, D. M., Davis, M. W., Avery, L., and Bargmann, C. I. (2002). Social feeding in Caenorhabditis elegans is induced by neurons that detect aversive stimuli. Nature *419*, 899-903.
Denninger, J. W., and Marletta, M. A. (1999). Guanylate cyclase and the •NO/cGMP signaling pathway. Biochim Biophys Acta *1411*, 334-350.
Dent, J. A., Davis, M. W., and Avery, L. (1997). avr-15 encodes a chloride channel subunit that mediates inhibitory glutamatergic neurotransmission and ivermectin sensitivity in Caenorhabditis elegans. Embo J *16*, 5867-5879.
Dent, J. A., Smith, M. M., Vassilatis, D. K., and Avery, L. (2000). The genetics of ivermectin resistance in Caenorhabditis elegans. Proc Natl Acad Sci U S A *97*, 2674-2679.
Di Iorio, E. E. (1981). Preparation of derivatives of ferrous and ferric hemoglobin. In Hemoglobins, E. Antonini, L. Rossi-Bernardi, and E. Chiancone, eds. (New York, Academic Press), pp. 57-71.
Duffy, D. C., McDonald, J. C., Schueller, O. J. A., and Whitesides, G. M. (1998). Rapid prototyping of microfluidic systems in poly(dimethylsiloxane). Anal Chem *70*, 4974-4984.
Dusenbery, D. B. (1980). Appetitive response of the nematode *Caenorhabditis elegans* to oxygen. J Comp Physiol *136*, 333-336.
Faber, D. S., and Korn, H. (1978). Neurobiology of the Mauthner cell (New York, Raven Press).
Finn, J. T., Grunwald, M. E., and Yau, K. W. (1996). Cyclic nucleotide-gated ion channels: an extended family with diverse functions. Annu Rev Physiol *58*, 395-426.
Fujiwara, M., Sengupta, P., and McIntire, S. L. (2002). Regulation of body size and behavioral state of C. elegans by sensory perception and the EGL-4 cGMP-dependent protein kinase. Neuron *36*, 1091-1102.
Garcia, L. R., Mehta, P., and Sternberg, P. W. (2001). Regulation of distinct muscle behaviors controls the C. elegans male's copulatory spicules during mating. Cell *107*, 777-788.
Gibb, B. J., Wykes, V., and Garthwaite, J. (2003). Properties of NO-activated guanylyl cyclases expressed in cells. Br J Pharmacol *139*, 1032-1040.
Gilles-Gonzalez, M. A., Gonzalez, G., and Perutz, M. F. (1994). Heme-based sensors, exemplified by the kinase FixL, are a new class of heme protein with distinctive ligand binding and autoxidation. Biochemistry *33*, 8067-8073.
Gomez, M., De Castro, E., Guarin, E., Sasakura, H., Kuhara, A., Mori, I., Bartfai, T., Bargmann, C. I., and Nef, P. (2001). Ca2+ signaling via the neuronal calcium sensor-1 regulates associative learning and memory in C. elegans. Neuron *30*, 241-248.
Gong, W., Hao, B., Mansy, S. S., Gonzalez, G., Gilles-Gonzalez, M. A., and Chan, M. K. (1998). Structure of a biological oxygen sensor: a new mechanism for heme-driven signal transduction. Proc Natl Acad Sci U S A *95*, 15177-15182.
Hart, A. C., Sims, S., and Kaplan, J. M. (1995). Synaptic code for sensory modalities revealed by C. elegans GLR-1 glutamate receptor. Nature *378*, 82-85.

Hedgecock, E. M., and Russell, R. L. (1975). Normal and mutant thermotaxis in the nematode Caenorhabditis elegans. Proc Natl Acad Sci U S A *72*, 4061-4065.
Hieb, W. F., Stokstad, E. L., and Rothstein, M. (1970). Heme requirement for reproduction of a free-living nematode. Science *168*, 143-144.
Hilliard, M. A., Bargmann, C. I., and Bazzicalupo, P. (2002). C. elegans Responds to Chemical Repellents by Integrating Sensory Inputs from the Head and the Tail. Curr Biol *12*, 730-734.
Hilliard, M. A., Bergamasco, C., Arbucci, S., Plasterk, R. H., and Bazzicalupo, P. (2004). Worms taste bitter: ASH neurons, QUI-1, GPA-3 and ODR-3 mediate quinine avoidance in Caenorhabditis elegans. Embo J *23*, 1101-1111.
Hills, T., Brockie, P. J., and Maricq, A. V. (2004). Dopamine and glutamate control area-restricted search behavior in Caenorhabditis elegans. J Neurosci *24*, 1217-1225.
Hornbein, T. F. (1981). Regulation of breathing (New York, M. Dekker).
Hou, S., Larsen, R. W., Boudko, D., Riley, C. W., Karatan, E., Zimmer, M., Ordal, G. W., and Alam, M. (2000). Myoglobin-like aerotaxis transducers in Archaea and Bacteria. Nature *403*, 540-544.
Imlay, J. A. (2003). Pathways of oxidative damage. Annu Rev Microbiol *57*, 395-418.
Ishihara, T., Iino, Y., Mohri, A., Mori, I., Gengyo-Ando, K., Mitani, S., and Katsura, I. (2002). HEN-1, a secretory protein with an LDL receptor motif, regulates sensory integration and learning in Caenorhabditis elegans. Cell *109*, 639-649.
Jain, R., and Chan, M. K. (2003). Mechanisms of ligand discrimination by heme proteins. J Biol Inorg Chem *8*, 1-11.
Kaplan, J. M., and Horvitz, H. R. (1993). A dual mechanosensory and chemosensory neuron in Caenorhabditis elegans. Proc Natl Acad Sci U S A *90*, 2227-2231.
Karow, D. S., Pan, D., Tran, R., Pellicena, P., Presley, A., Mathies, R. A., and Marletta, M. A. (2004). Spectroscopic Characterization of the sGC-like heme domains from *Vibrio cholerae* and *Thermoanaerobacter tengcongensis*. Biochemistry *In Press*.
Koglin, M., Vehse, K., Budaeus, L., Scholz, H., and Behrends, S. (2001). Nitric oxide activates the b2 subunit of soluble guanylyl cyclase in the absence of a second subunit. J Biol Chem *276*, 30737-30743.
Komatsu, H., Mori, I., Rhee, J. S., Akaike, N., and Ohshima, Y. (1996). Mutations in a cyclic nucleotide-gated channel lead to abnormal thermosensation and chemosensation in C. elegans. Neuron *17*, 707-718.
Lee, R. Y., Sawin, E. R., Chalfie, M., Horvitz, H. R., and Avery, L. (1999). EAT-4, a homolog of a mammalian sodium-dependent inorganic phosphate cotransporter, is necessary for glutamatergic neurotransmission in caenorhabditis elegans. J Neurosci *19*, 159-167.
Liu, K. S., and Sternberg, P. W. (1995). Sensory regulation of male mating behavior in Caenorhabditis elegans. Neuron *14*, 79-89.
Loer, C. M., and Kenyon, C. J. (1993). Serotonin-deficient mutants and male mating behavior in the nematode Caenorhabditis elegans. J Neurosci *13*, 5407-5417.
Lopez-Barneo, J. (2003). Oxygen and glucose sensing by carotid body glomus cells. Curr Opin Neurobiol *13*, 493-499.
Lopez-Barneo, J., Pardal, R., and Ortega-Saenz, P. (2001). Cellular mechanism of oxygen sensing. Annu Rev Physiol *63*, 259-287.

Maines, M. D., and Gibbs, P. E. (2005). 30 some years of heme oxygenase: from a "molecular wrecking ball" to a "mesmerizing" trigger of cellular events. Biochem Biophys Res Commun *338*, 568-577.
Malinski, T., and Taha, Z. (1992). Nitric oxide release from a single cell measured in situ by a porphyrinic-based microsensor. Nature *358*, 676-678.
Malinski, T., Taha, Z., and Grunfeld, S. (1993). Diffusion of nitric oxide in the aorta wall monitored in situ by porphyrinic microsensors. Biochem Biophys Res Comm *193*, 1076-1082.
Maricq, A. V., Peckol, E., Driscoll, M., and Bargmann, C. I. (1995). Mechanosensory signalling in C. elegans mediated by the GLR-1 glutamate receptor. Nature *378*, 78-81.
McIntire, S. L., Jorgensen, E., Kaplan, J., and Horvitz, H. R. (1993). The GABAergic nervous system of Caenorhabditis elegans. Nature *364*, 337-341.
Mellem, J. E., Brockie, P. J., Zheng, Y., Madsen, D. M., and Maricq, A. V. (2002). Decoding of polymodal sensory stimuli by postsynaptic glutamate receptors in C. elegans. Neuron *36*, 933-944.
Mello, C., and Fire, A. (1995). DNA transformation. Methods Cell Biol *48*, 451-482.
Monson, E. K., Weinstein, M., Ditta, G. S., and Helinski, D. R. (1992). The FixL protein of Rhizobium meliloti can be separated into a heme-binding oxygen-sensing domain and a functional C-terminal kinase domain. Proc Natl Acad Sci USA *89*, 4280-4284.
Mori, I., and Ohshima, Y. (1995). Neural regulation of thermotaxis in Caenorhabditis elegans. Nature *376*, 344-348.
Morton, D. B. (2004a). Atypical soluble guanylyl cyclases in Drosophila can function as molecular oxygen sensors. J Biol Chem *279*, 50651-50653.
Morton, D. B. (2004b). Invertebrates yield a plethora of atypical guanylyl cyclases. Mol Neurobiol *29*, 97-116.
Morton, D. B., Hudson, M. L., Waters, E., and O'Shea, M. (1999). Soluble guanylyl cyclases in Caenorhabditis elegans: NO is not the answer. Curr Biol *9*, R546-547.
Nurse, C. A., and Fearon, I. M. (2002). Carotid body chemoreceptors in dissociated cell culture. Microsc Res Tech *59*, 249-255.
Nusbaum, M. P., and Beenhakker, M. P. (2002). A small-systems approach to motor pattern generation. Nature *417*, 343-350.
Pellicena, P., Karow, D. S., Boon, E. M., Marletta, M. A., and Kuriyan, J. (2004). Crystal structure of an oxygen-binding heme domain related to soluble guanylate cyclases. Proc Natl Acad Sci U S A *101*, 12854-12859.
Perkins, L. A., Hedgecock, E. M., Thomson, J. N., and Culotti, J. G. (1986). Mutant sensory cilia in the nematode Caenorhabditis elegans. Dev Biol *117*, 456-487.
Pierce-Shimomura, J. T., Morse, T. M., and Lockery, S. R. (1999). The fundamental role of pirouettes in Caenorhabditis elegans chemotaxis. J Neurosci *19*, 9557-9569.
Prabhakar, N. R. (2005). Oxygen Sensing at the Carotid Body: Why Multiple O2 Sensors and Multiple Transmitters? Exp Physiol.
Ranganathan, R., Cannon, S. C., and Horvitz, H. R. (2000). MOD-1 is a serotonin-gated chloride channel that modulates locomotory behaviour in C. elegans. Nature *408*, 470-475.
Rankin, C. H. (1991). Interactions between two antagonistic reflexes in the nematode Caenorhabditis elegans. J Comp Physiol [A] *169*, 59-67.

Rankin, C. H., Gannon, T., and Wicks, S. R. (2000). Developmental analysis of habituation in the Nematode C. elegans. Dev Psychobiol *36*, 261-270.
Rankin, C. H., and Wicks, S. R. (2000). Mutations of the caenorhabditis elegans brain-specific inorganic phosphate transporter eat-4 affect habituation of the tap-withdrawal response without affecting the response itself. J Neurosci *20*, 4337-4344.
Ren, P., Lim, C. S., Johnsen, R., Albert, P. S., Pilgrim, D., and Riddle, D. L. (1996). Control of C. elegans larval development by neuronal expression of a TGF-beta homolog. Science *274*, 1389-1391.
Reyrat, J. M., David, M., Blonski, C., Boistard, P., and Batut, J. (1993). Oxygen-regulated in vitro transcription of Rhizobium meliloti nifA and fixK genes. J Bacteriol *175*, 6867-6872.
Rodgers, K. R. (1999). Heme-based sensors in biological systems. Curr Opin Chem Biol *3*, 158-167.
Rogers, C., Reale, V., Kim, K., Chatwin, H., Li, C., Evans, P., and de Bono, M. (2003). Inhibition of *Caenorhabditis elegans* social feeding by FMRFamide-related peptide activation of NPR-1. Nat Neurosci *6*, 1178-1185.
Russwurm, M., Behrends, S., Harteneck, C., and Koesling, D. (1998). Functional properties of a naturally occurring isoform of soluble guanylyl cyclase. Biochem J *335*, 125-130.
Ryu, W. S., and Samuel, A. D. (2002). Thermotaxis in Caenorhabditis elegans analyzed by measuring responses to defined Thermal stimuli. J Neurosci *22*, 5727-5733.
Sambongi, Y., Nagae, T., Liu, Y., Yoshimizu, T., Takeda, K., Wada, Y., and Futai, M. (1999). Sensing of cadmium and copper ions by externally exposed ADL, ASE, and ASH neurons elicits avoidance response in Caenorhabditis elegans. Neuroreport *10*, 753-757.
Sawin, E. R., Ranganathan, R., and Horvitz, H. R. (2000). C. elegans locomotory rate is modulated by the environment through a dopaminergic pathway and by experience through a serotonergic pathway. Neuron *26*, 619-631.
Schackwitz, W. S., Inoue, T., and Thomas, J. H. (1996). Chemosensory neurons function in parallel to mediate a pheromone response in C. elegans. Neuron *17*, 719-728.
Schafer, W. R., Sanchez, B. M., and Kenyon, C. J. (1996). Genes affecting sensitivity to serotonin in Caenorhabditis elegans. Genetics *143*, 1219-1230.
Semenza, G. L. (2000). HIF-1: mediator of physiological and pathophysiological responses to hypoxia. J Appl Physiol *88*, 1474-1480.
Semenza, G. L. (2001). HIF-1, O(2), and the 3 PHDs: how animal cells signal hypoxia to the nucleus. Cell *107*, 1-3.
Shyn, S. I., Kerr, R., and Schafer, W. R. (2003). Serotonin and Go modulate functional states of neurons and muscles controlling C. elegans egg-laying behavior. Curr Biol *13*, 1910-1915.
Stone, J. R., and Marletta, M. A. (1994). Soluble Guanylate Cyclase from Bovine Lung: Activation with Nitric Oxide and Carbon Monoxide and Spectral Characterization of the Ferrous and Ferric States. Biochemistry *33*, 5636-5640.
Sulston, J. E., Albertson, D. G., and Thomson, J. N. (1980). The Caenorhabditis elegans male: postembryonic development of nongonadal structures. Dev Biol *78*, 542-576.
Sunahara, R. K., Beuve, A., Tesmer, J. J., Sprang, S. R., Garbers, D. L., and Gilman, A. G. (1998). Exchange of substrate and inhibitor specificities between adenylyl and guanylyl cyclases. J Biol Chem *273*, 16332-16338.

Sylvia, D. M. (1998). Principles and applications of soil microbiology (Upper Saddle River, N.J., Prentice Hall).
Sze, J. Y., Victor, M., Loer, C., Shi, Y., and Ruvkun, G. (2000). Food and metabolic signalling defects in a Caenorhabditis elegans serotonin-synthesis mutant. Nature *403*, 560-564.
Tabish, M., Siddiqui, Z. K., Nishikawa, K., and Siddiqui, S. S. (1995). Exclusive expression of C. elegans osm-3 kinesin gene in chemosensory neurons open to the external environment. J Mol Biol *247*, 377-389.
Tanouye, M. A., and Wyman, R. J. (1980). Motor outputs of giant nerve fiber in Drosophila. J Neurophysiol *44*, 405-421.
Tesmer, J. J., Sunahara, R. K., Gilman, A. G., and Sprang, S. R. (1997). Crystal structure of the catalytic domains of adenylyl cyclase in a complex with Gsalpha.GTPgammaS. Science *278*, 1907-1916.
Troemel, E. R., Kimmel, B. E., and Bargmann, C. I. (1997). Reprogramming chemotaxis responses: sensory neurons define olfactory preferences in C. elegans. Cell *91*, 161-169.
Tsalik, E. L., and Hobert, O. (2003). Functional mapping of neurons that control locomotory behavior in Caenorhabditis elegans. J Neurobiol *56*, 178-197.
Van Voorhies, W. A., and Ward, S. (2000). Broad oxygen tolerance in the nematode Caenorhabditis elegans. J Exp Biol *203 Pt 16*, 2467-2478.
Waggoner, L. E., Zhou, G. T., Schafer, R. W., and Schafer, W. R. (1998). Control of alternative behavioral states by serotonin in Caenorhabditis elegans. Neuron *21*, 203-214.
Wakabayashi, T., Kitagawa, I., and Shingai, R. (2004). Neurons regulating the duration of forward locomotion in Caenorhabditis elegans. Neurosci Res *50*, 103-111.
Wallace, H. R. (1969). Nematologica *15*, 75-89.
Wannamaker, C. M., and Rice, J. A. (2000). Effects of hypoxia on movements and behavior of selected estuarine organisms from the southeastern United States. *249*, 145-163.
Ward, S. (1973). Chemotaxis by the nematode Caenorhabditis elegans: identification of attractants and analysis of the response by use of mutants. Proc Natl Acad Sci U S A *70*, 817-821.
White, J., Southgate, E., Thomson, J.N., and Brenner, S. (1986). The structure of the nervous system of the namatode Caenorhabditis elegans. Philos Trans R Soc Lond B Biol Sci *314*, 1-340.
Whittaker, A. J., and Sternberg, P. W. (2004). Sensory processing by neural circuits in Caenorhabditis elegans. Curr Opin Neurobiol *14*, 450-456.
Wicks, S. R., Roehrig, C. J., and Rankin, C. H. (1996). A dynamic network simulation of the nematode tap withdrawal circuit: predictions concerning synaptic function using behavioral criteria. J Neurosci *16*, 4017-4031.
Williams, S. E., Wootton, P., Mason, H. S., Bould, J., Iles, D. E., Riccardi, D., Peers, C., and Kemp, P. J. (2004). Hemoxygenase-2 is an oxygen sensor for a calcium-sensitive potassium channel. Science *306*, 2093-2097.
Wingrove, J. A., and O'Farrell, P. H. (1999). Nitric oxide contributes to behavioral, cellular, and developmental responses to low oxygen in Drosophila. Cell *98*, 105-114.
Wu, R. S. (2002). Hypoxia: from molecular responses to ecosystem responses. Mar Pollut Bull *45*, 35-45.

Yu, S., Avery, L., Baude, E., and Garbers, D. L. (1997). Guanylyl cyclase expression in specific sensory neurons: a new family of chemosensory receptors. Proc Natl Acad Sci U S A *94*, 3384-3387.
Zariwala, H. A., Miller, A. C., Faumont, S., and Lockery, S. R. (2003). Step response analysis of thermotaxis in Caenorhabditis elegans. J Neurosci *23*, 4369-4377.
Zhang, Y., Lu, H., and Bargmann, C. I. (2005). Pathogenic bacteria induce aversive olfactory learning in Caenorhabditis elegans. Nature *438*, 179-184.
Zhao, B., Khare, P., Feldman, L., and Dent, J. A. (2003). Reversal frequency in Caenorhabditis elegans represents an integrated response to the state of the animal and its environment. J Neurosci *23*, 5319-5328.
Zhao, Y., and Marletta, M. A. (1997). Localization of the heme binding region in soluble guanylate cyclase. Biochemistry *36*, 15959-15964.
Zheng, Y., Brockie, P. J., Mellem, J. E., Madsen, D. M., and Maricq, A. V. (1999). Neuronal control of locomotion in C. elegans is modified by a dominant mutation in the GLR-1 ionotropic glutamate receptor. Neuron *24*, 347-361.

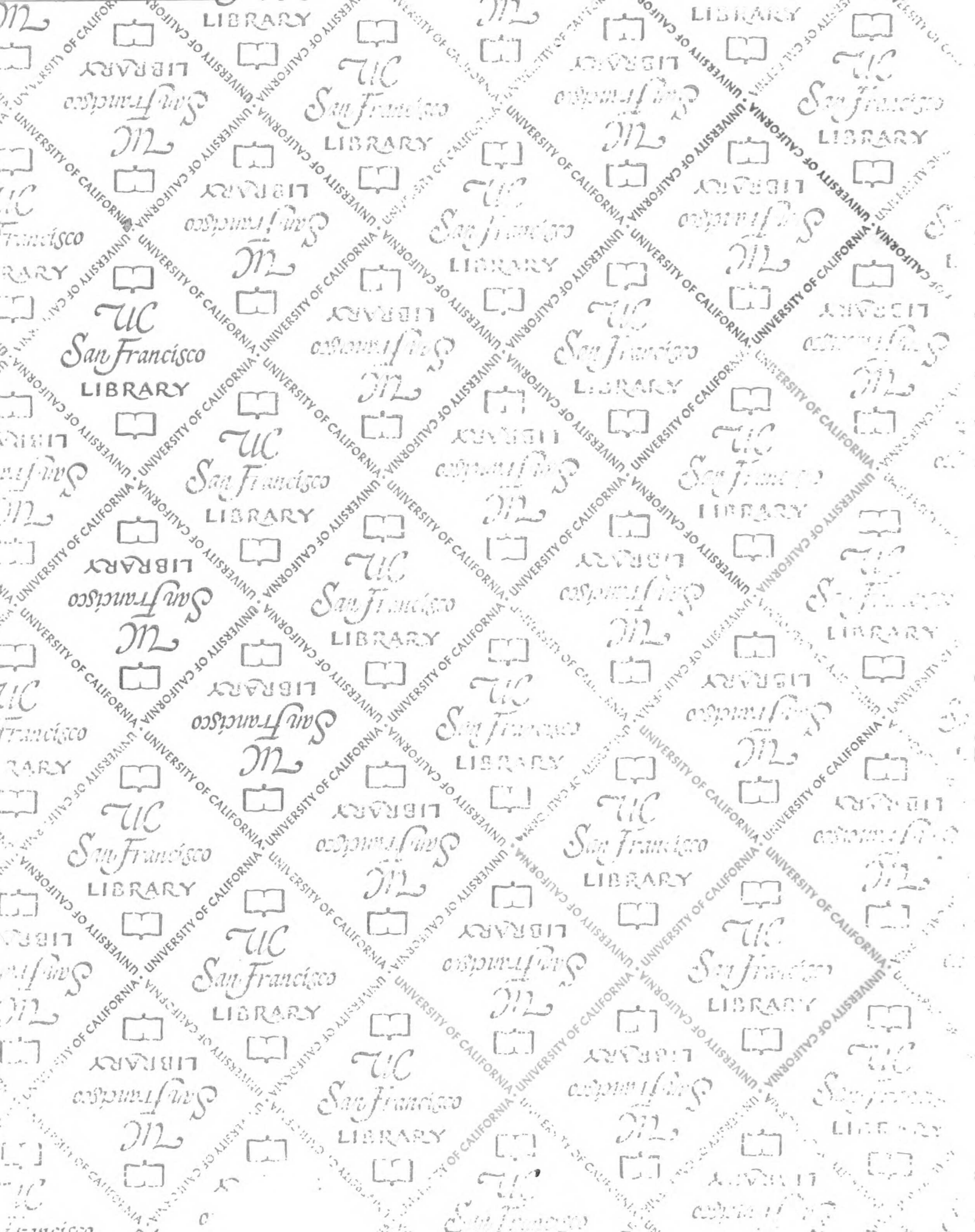
UC
San Francisco
LIBRARY
UNIVERSITY OF CALIFORNIA · UNIVERSITY OF CALIFORNIA

For reference

Not to be taken from the room.